Molecular Pharmacology Fast Forward. Published on October 23, 2015 as DOI: 10.1124/mol.115.100792
This article has not been copyedited and formatted. The final version may differ from this version.

Title Page

Identification and validation of larixyl acetate as a potent TRPC6 inhibitor

Nicole Urban, Liming Wang, Sandra Kwiek, Jörg Rademann,

Wolfgang M. Kuebler, and Michael Schaefer

Rudolf-Boehm-Institut für Pharmakologie und Toxikologie, Universität Leipzig, Leipzig, Germany (N.U. and M.S.); Institut für Pharmazie, Freie Universität Berlin, Berlin, Germany (S.K. and J.R.); and St. Michael´s Hospital, The Keenan Research Centre, Toronto, Canada (L.W. and W.K.)

Molecular Pharmacology Fast Forward. Published on October 23, 2015 as DOI: 10.1124/mol.115.100792
This article has not been copyedited and formatted. The final version may differ from this version.

Running Title Page

Running title:

Larixyl acetate is a TRPC6 inhibitor

Send correspondence to:

Prof. Dr. Michael Schaefer

Universität Leipzig

Rudolf-Boehm-Institut für Pharmakologie und Toxikologie

Härtelstraße 16-18

04107 Leipzig, Germany

Tel: +49-341-9724600, Fax: +49-341-9724609

E-mail: michael.schaefer@medizin.uni-leipzig.de

Document statistics:

21 text pages

1 table

11 figures

42 references

266 words in the Abstract

589 words in the Introduction

1334 words in the Discussion

List of abbreviations:

COPD, chronic obstructive pulmonary disease; DAG, diacylglycerol; DMSO, dimethyl-sulfoxide; GPCR, G protein-coupled receptor; HEK, human embryonic kidney; HPV, hypoxia-induced pulmonary vasoconstriction; IC_{50}, half maximal inhibitory concentration; OAG, 1-oleoyl-2-acetyl-*sn*-glycerol; PASMC, pulmonary artery smooth muscle cells; TRP, transient receptor potential; TRPC, classical or canonical TRP channel

Molecular Pharmacology Fast Forward. Published on October 23, 2015 as DOI: 10.1124/mol.115.100792
This article has not been copyedited and formatted. The final version may differ from this version.

Abstract

TRPC6, a non-selective and Ca^{2+}-permeable cation channel, mediates pathophysiological responses within pulmonary and renal diseases that are still poorly controlled by current medication. Thus, controlling TRPC6 activity may provide a promising and challenging pharmacological approach. Recently identified chemical entities have demonstrated that TRPC6 is pharmacologically targetable. However, isotype-selectivity with regard to its closest relative, TRPC3 is difficult to achieve. Reasoning that balsams, essential oils or incense materials that are traditionally used for inhalation may contain biological activities to block TRPC6 activity, we embarked on a natural compound strategy to identify new TRPC6-blocking chemical entities. Within several preparations of plant extracts, a strong TRPC6-inhibitory activity was found in conifer balsams. The biological activity was associated with the non-volatile resins, but not with the essential oils. Of various conifers, the larch balsam was unique in displaying a marked TRPC6-prevalent mode of action. By testing the main constituents of larch resin, we identified larixol and larixyl acetate as blockers of Ca^{2+} entry and ionic currents through diacylglycerol- or receptor-activated recombinant TRPC6 channels, exhibiting an about 12-fold and 5-fold selectivity compared to its closest relatives TRPC3 and TRPC7, respectively. No significant inhibition of more distantly related TRPV or TRPM channels was seen. The potent inhibition of recombinant TRPC6 by larixyl acetate (IC_{50} = 0.1-0.6 μM) was confirmed for native TRPC6-like $[Ca^{2+}]_i$ signals in diacylglycerol-stimulated rat pulmonary artery smooth muscle cells (PASMC). In isolated mouse lungs, larix-6-yl monoacetate (CAS 4608-49-5; larixyl acetate; 5 μM) prevented the acute hypoxia-induced vasoconstriction. We conclude that larch-derived labdane-type diterpenes are TRPC6-selective inhibitors and may represent a starting point for pharmacological TRPC6 modulation within experimental therapies.

Molecular Pharmacology Fast Forward. Published on October 23, 2015 as DOI: 10.1124/mol.115.100792
This article has not been copyedited and formatted. The final version may differ from this version.

Introduction

Classical or canonical TRP channels (TRPC) are second messenger-gated, Ca^{2+}-permeable cation channels that are activated in a receptor- and phospholipase C-dependent mechanism (Ong et al. 2014). A closely related subgroup consisting of TRPC3, TRPC6 and TRPC7 shares the unique property of being directly activated by diacylglycerols (DAG) (Hofmann et al. 1999). Within the context of ligand-induced signalling events, DAG is mainly formed by PI-specific phospholipases that cleave phosphatidylinositol-4,5-bisphosphate to generate DAG and inositol-1,4,5-trisphosphate (InsP3). The endogenously formed DAG serves as a plasma membrane-localized lipid second messenger to recruit conventional and novel protein kinases C or other C1 domain-bearing signalling proteins, but also to activate the DAG-sensitive TRPC3/-6/-7 subgroup of TRPC channels (Gudermann et al. 2004; Hofmann et al. 1999; Okada et al. 1999). Membrane-permeable DAG analogues, such as 1-oleoyl-2-acetyl-*sn*-glycerol (OAG) and 1,2-dioctanoylglycerol (DOG) can substitute for the endogenously formed DAG species in triggering Na^+, K^+ and Ca^{2+} currents through TRPC6.

The expression of TRPC channels is widespread, but markedly differs between the isoforms. Therefore, selective blockers that modulate the activity of distinct isoforms or subgroups of TRPC isoforms are expected to exert a tissue-specific inhibition of receptor-triggered cellular Ca^{2+} influx and plasma membrane depolarisation. TRPC6 is expressed in vascular and airway smooth muscle cells (Dietrich et al. 2006; Wang et al. 2011; Welsh et al. 2002) and contributes to the vasoconstrictor response either by mediating receptor- and second messenger-triggered Ca^{2+} influx, or by depolarising the smooth muscle cell, resulting in the opening of voltage-gated Ca^{2+} channels. In the pulmonary vascular system, TRPC6 has gained considerable attention by several studies that demonstrated its involvement in hypoxia-induced pulmonary vasoconstriction (Fuchs et al. 2011; Tabeling et al. 2015; Weissmann et al. 2006) and in idiopathic pulmonary hypertension (Yu et al. 2004; Yu et al. 2009), but also by contributing to lung edema formation (Samapati et al. 2012; Weissmann et al. 2012). In addition, TRPC6 expression in lung macrophages (Finney-Hayward et al. 2010) and in bronchial smooth muscle cells may provide a link between TRPC6 and pathophysiological mechanisms that induce or aggravate chronic or allergic obstructive airway diseases (Sel et al. 2008).

In the kidney, TRPC6 is expressed in podocytes that constitute the glomerular filtration membranes (Reiser et al. 2005). Since non-synonymous mutations in the TRPC6 gene are

Molecular Pharmacology Fast Forward. Published on October 23, 2015 as DOI: 10.1124/mol.115.100792
This article has not been copyedited and formatted. The final version may differ from this version.

associated with focal segmental glomerulosclerosis, genetic and functional evidence points to a seminal contribution in controlling the integrity of the filtration slit (Reiser et al. 2005; Winn et al. 2005). Hence, pharmacological modulators that potently and efficiently block TRPC6 and may provide a biological tool to validate the role of TRPC6 in pulmonary and renal diseases, and to establish experimental therapies are intensely sought for.

Recently, we could demonstrate the general feasibility to identify inhibitors of human TRPC6, applying academic high-throughput-screening of a chemically diverse library (Urban et al. 2012). The resulting modulators, however, display only a limited preference to inhibit TRPC6 compared to its closest relatives, TRPC3 and TRPC7. Similarly, the biological activity of norgestimate to block DAG-sensitive TRPC channels does not markedly discriminate between single members of the TRPC3/6/7 subfamily (Miehe et al. 2012). We, therefore, embarked on another approach, applying natural extracts to identify compound mixtures that exert a TRPC6-prevalent biological activity, followed by narrowing down the fractions and candidate compounds to finally pinpoint the small molecules larixol and larix-6-yl monoacetate (CAS 4608-49-5; termed as larixyl acetate in this manuscript) as potent and selective TRPC6 blockers. Validation of the labdane-type diterpenes included the assessment of their selectivity, cytotoxicity, electrophysiological properties, and confirmation of the biological activity in endogenously TRPC6-expressing cells and tissues.

Molecular Pharmacology Fast Forward. Published on October 23, 2015 as DOI: 10.1124/mol.115.100792
This article has not been copyedited and formatted. The final version may differ from this version.

Materials and Methods

Materials

Essential oils were ordered from Neumond (Raisting, Germany), larch oil was purchased from Bauer & Cie. (Munich, Germany). All resins, turpentines and balsams were obtained from Kremer Pigmente (Aichstetten, Germany) and dissolved in DMSO in due consideration of their density. Abietic acid, neoabietic acid and isopimaric acid were from Sigma Aldrich (Germany), and pimaric acid from MP Biomedicals (Illkirch, France). For secondary screening, 13-epimanool and larixyl acetate were purchased from Seqchem Sequoia Research (Pangbourne, UK). All following experiments were conducted with larixol isolated and crystallized from *Larix decidua* turpentine following to treatment with KOH in order to saponify all contained esters. Larix-6-yl monoacetate was obtained from larixol by acetylation with acetic anhydride and chromatographic purification. Identity and purity of both larixol and larix-6-yl monoacetate were confirmed by ^{1}H- and ^{13}C-NMR spectroscopy and by high resolution MS (Supplemental Figures 1 and 2).

Cell culture and transfections

Parental and stably transfected HEK293 cells were cultured in Earle´s Minimum Essential Medium (MEM), supplemented with 10% fetal calf serum (Biochrom), 2 mM L-glutamine, 100 U/ml penicillin, and 0.1 mg/ml streptomycin. To generate stably transfected cell lines, HEK293 cells were seeded in 35-mm culture dishes, and transfected with 4 µl Fugene HD (Roche) and 2 µg of DNA encoding human TRPC3-YFP, mouse TRPC4ß-YFP, human TRPC6-YFP, human TRPC7-YFP, rat TRPV1:YFP, mTRPV4-YFP or human TRPM8-CFP. Human TRPC7 (kind gift from Masayuki Mori, Fukuoka, Japan) was subcloned into a custom-made pcDNA3-YFP vector with the stop codon replaced by an in-frame ligatable Not-I restriction site. Stably transfected colonies were obtained in the presence of 1 mg/ml geneticin (G418) with a limiting dilution method. Inducible HEK293$_{mTRPC5\text{-}YFP}$ cell lines were maintained and induced as recently described (Richter et al. 2013). The HEK293$_{mTRPM3\alpha2}$ cell line was kindly provided by Johannes Oberwinkler, Marburg, Germany.

For PKCε translocation assays, a stable HEK293YFP-rPKCε cell line (Lent et al. 2002) was seeded on 25-mm glass coverslips for subsequent confocal (LSM 510, Carl Zeiss, Jena, Germany) imaging. Voltage-gated calcium channels ($Ca_V1.2$) were heterologously expressed as described (Romanin et al. 2000) by co-transfecting HEK293 cells in 35-mm dishes with

Molecular Pharmacology Fast Forward. Published on October 23, 2015 as DOI: 10.1124/mol.115.100792
This article has not been copyedited and formatted. The final version may differ from this version.

the following plasmids: pcDNA3-$\alpha 1_{c77}$ (0.5 µg/well), pcDNA3-β_{2a} (0.8 µg/well), pcDNA3-$\alpha_{2\delta}$ (0.7 µg/well), pEYFP-C1 (0.2 µg/well) for visualization. Cells were maintained at 37°C and in a 5% CO_2-aerated humidified atmosphere.

Ca^{2+} measurements in multiwell plates

Unless otherwise stated, Ca^{2+} assays were performed in HEPES-buffers saline (HBS), containing 132 mM NaCl, 6 mM KCl, 1 mM $MgCl_2$, 1mM $CaCl_2$, 5.5 mM D-glucose, and 10 mM HEPES adjusted to pH 7.4 with NaOH. When Ca^{2+} influx was induced by OAG, the buffer was supplemented with 0.03% bovine serum albumin (BSA). $HEK293_{TRP}$ cell lines were grown to confluence in 75-cm^2 flasks, detached with 0.25% trypsin, and loaded in culture medium with 4 µM fluo-4/AM (Invitrogen) for 30 min at 37°C. After washing (100 x g; 3 min), cells were resuspended in HBS, and dispensed into pigmented clear-bottom 384-well plates (Corning, USA; 36 µl/well). In case of GPCR stimulation the HBS contained 2 µM thapsigargin to deplete internal inositol-1,4,5-trisphosphate-sensitive Ca^{2+} stores. Measurements were carried out in a two-step protocol using a custom-made fluorescence imaging plate reader (FLIPR) built into a robotic liquid handling station (Freedom Evo 150, Tecan, Switzerland). Fluo 4 was excited at 450-470 nm with an LED array, filtered with a 475 nm short-pass filter (DT-blue; Optics Balzers, Balzers, Liechtenstein), and emitted fluorescence was imaged with a cooled CCD camera (Coolsnap FX, Photometrics, Tucson, AZ), equipped with a Xenon 0.95/25 C-mount lens (Schneider Kreuznach, Bad Kreuznach, Switzerland) and a 515 nm long-pass filter (Y515-Di; Fujifilm, Tokyo, Japan). Compounds were added at the indicated final concentrations during the recording, and incubated for 5 minutes. In a second time-lapse analysis, cells were stimulated with the respective agonist. During injections, fluorescence images were continuously monitored under control of the Micromanager software (Edelstein et al., 2010). Fluorescence intensities in single wells were calculated with ImageJ software (Abramoff et al., 2004), corrected for the respective background signals and normalized to the initial intensities (F/F_0). Concentration response curves were generated by Hill equation fits. The activators were 50 µM OAG for TRPC3, TRPC6 and TRPC7, 2 µM capsaicin for TRPV1, 10 nM GSK1016790A for TRPV4, 1mM H_2O_2 for TRPM2, 30 µM pregnenolone sulfate for TRPM3α2; and 300 µM menthol for TRPM8. GPCR-mediated activation of TRPC4ß, TRPC5 and TRPC6 was achieved with a mix of 1 mM carbachol, 300 µM ATP, and 0.5 U/ml thrombin. Activation of TRP channels was

Molecular Pharmacology Fast Forward. Published on October 23, 2015 as DOI: 10.1124/mol.115.100792
This article has not been copyedited and formatted. The final version may differ from this version.

measured as increasing intracellular calcium concentrations in the form of rising fluo-4 fluorescence intensities or as loss of co-expressed YFP fluorescence by acidification in $HEK293_{rTRPV1:YFP}$ cells. Note, if detachment of cells resulted in an impaired apparent channel activity, adherent cells (20,000 cells per well) were grown and loaded with Fluo-4 in tissue culture-treated 384-well plates (Greiner, Germany), and experiments were carried out with monolayers.

PKCε translocation

Coverslips with adherently growing $HEK293_{PKCε\text{-}YFP}$ cells (Schaefer et al. 2001) were placed in chamber containing HBS with or without 10 µM larixyl actetate and mounted onto the stage of an inverted LSM510-META confocal microscope. Imaging was performed with excitation at 514 nm and emission filtered with a 530-nm long pass filter. A Plan-Apochromat 100x/1.46 objective was used, and pinholes were set to yield optical slices with a thickness of 0.6-0.8 µm. After an incubation of 5 minutes, visual fields with 5-12 cells were selected, and the PKCε-YFP distribution was imaged over the time. Activation of PKCε-YFP was triggered by adding 1 mM carbachol, 300 µM ATP, and 0.5 U/ml thrombin to the bath solution. For statistical analysis, regions of interest were defined in cytoplasmic areas of single cells, and PKCε-YFP translocation was examined in consideration of background and bleaching controls. Finally, data were normalized to initial cytosolic PKCε-YFP intensity.

Electrophysiological procedures

Whole cell and single channel patch clamp analysis were performed at room temperature using a Multiclamp 700B amplifier with a Digidata 1440A digitizer (Axon CNS, Molecular Devices) controlled with the PClamp 10 software (Molecular Devices). $HEK293_{hTRPC6\text{-}YFP}$, $HEK293_{hTRPC3\text{-}YFP}$ and PASM cells were seeded at low density on glass coverslips 6-24 hours before the experiments. Coverslips were mounted in a perfused chamber (Warner Instruments) placed on the stage of an inverted microscope. The standard extracellular solution contained 140 mM NaCl, 5 mM CsCl, 2 mM $MgCl_2$, 1 mM $CaCl_2$, and 10 mM HEPES adjusted to pH 7.4 with NaOH. In case of stimulation with OAG, the bath solution additionally contained 0.1% BSA as well as 1 µM nifedipine and 1 µM BIM if PASM cells were examined. Patch pipettes were made from borosilicate glass (Science Products) and had a resistance of 4-8 MΩ when filled with the standard pipette solution: 140 mM CsCl, 4 mM $MgCl_2$, 10 mM

Molecular Pharmacology Fast Forward. Published on October 23, 2015 as DOI: 10.1124/mol.115.100792
This article has not been copyedited and formatted. The final version may differ from this version.

EGTA, and 10 mM HEPES adjusted to pH 7.2 with CsOH. In all whole-cell experiments, serial resistance was lower than 12 MΩ, and compensated by 70%. A modified pipette solution with 5 mM EGTA and 1.1 mM $CaCl_2$ (calculated free Ca^{2+} = 100 nM) was used when AlF_4^- infusion, inside-out, and outside-out experiments were carried out. For TRPC6 activation by 30 µM AlF_4^-, 500 µl of this pipette solution was freshly mixed with 10 µl of 0.5 M NaF and 2.5 µl of 6 mM $AlCl_3$, and filled in pipettes. To record current/voltage (I/V)-curves, voltage ramps from -100 mV to +100 mV with a slope of 400 mV s^{-1} were applied. All whole cell currents were filtered at 3 kHz (four-pole Bessel filter) and sampled at 10 kHz.

Electrophysiological measurements of recombinant CaV1.2

The bath solution contained 82 mM NaCl, 20 mM triethanolamine-Cl, 30 mM $BaCl_2$, 5 mM CsCl, 1 mM $MgCl_2$, 0.1 mM EGTA, 10 mM glucose, and 5 mM HEPES adjusted to pH 7.4 with NaOH. Intracellular solution was: 102 mM CsCl, 10 mM triethanolamine-Cl, 1 mM $MgCl_2$, 10 mM EGTA, 3 mM Na_2ATP, and 5 mM HEPES adjusted to pH 7.4 with CsOH. The voltage step protocol consisted of 300 ms pulses, stepping from a holding potential of -70 mV to -50 mV to +80 mV in increments of 10 mV. Inhibition of Cav1.2 was examined after incubation with the respective compounds for 200 s by applying a 300 ms test pulse to +20 mV, followed by a second test pulse 160 s after wash-out of the modulators. Maximum current amplitudes were determined in the presence of the modulators and after wash-out.

Detection of cytotoxicity and cell viability

Membrane integrity was assessed with a propidium iodide exclusion assay upon short (10 min) and long-term (24 h) incubation with the test compounds in HEK293 cell suspensions and adherent HEK293 cell cultures, respectively. After addition of 2 µg/ml propidium iodide, fluorescence signals were detected with excitation at 544 nm and emission at 620/10 nm in a plate reader device, followed by acute injection of Triton X-100 (0.2%) to obtain maximal intensities for normalisation.

To assess the cell viability, an MTT assay was executed. HEK293 cells were seeded in poly-L-lysine-coated 96-well cell culture plates at a density of 10^4 cells per well. Next day, medium was exchanged, and test compounds were incubated for another 24 hours. After removal of the medium, cells were incubated for 3 hours in fresh medium, containing 0.5 mg/ml MTT. Subsequently, supernatants were discarded, cells were lysed, and formed formazan crystals

Molecular Pharmacology Fast Forward. Published on October 23, 2015 as DOI: 10.1124/mol.115.100792
This article has not been copyedited and formatted. The final version may differ from this version.

were completely dissolved in 100% DMSO. Absorbance was detected at 560 nm and 670 nm (reference wavelength). Finally, differences of both extinctions were calculated. All measurements were executed with a multiwell plate reader (Polarstar Omega, BMG Labtech; Germany).

Compound stability in whole blood

Venous blood from healthy, adult donors was drawn and anticoagulated with trisodium citrate (1:10 vol/vol, 110 mM). After adding 100 µM larixyl actetate or 1% DMSO, samples were kept at 37°C, and aliquots were taken, centrifuged (2400 x g; 10 min), and citrate plasma was immediately frozen at -20°C. The biological activity to inhibit TRPC6 was assessed by intracellular Ca^{2+} measurements in $HEK293_{hTRPC6\text{-}YFP}$ cells as described above in the presence of 10% of the conditioned plasma samples (corresponding to a final larixyl acetate concentration of 10 µM). Due to an inactivating protein binding of OAG, stimulation with a GPCR agonist mix was performed (1 mM carbachol, 300 µM ATP, and 0.5 U/ml thrombin).

Smooth muscle cell isolation, immunofluorescence and Western blot

After thoracotomy of 3 week old rats, pulmonary arteries were dissected from generation one to fourth. The blood vessels were washed and mechanically cut in small pieces in a cold buffer containing 127 mM NaCl, 5.9 mM KCl, 1.2 mM $MgCl_2$, 2.4 mM $CaCl_2$, 1.8 mM glucose, and 10 mM HEPES adjusted to pH 7.4. Enzymatic digestion was done in a mix of one volume DMEM/Hams F12-solved papain (0.5 mg/ml, Sigma) and one volume of buffer without calcium but with additional 32 mM DTT, and 0.5% bovine albumin (Sigma) for 30 minutes at 37°C. Upon short centrifugation, supernatants were discarded, and pulmonary artery pieces were digested with a buffer containing 0.75 mg/ml collagenase (Sigma) in the presence of 0.5% bovine serum albumin for 10 minutes at 37°C. The enzyme was removed by centrifugation, and smooth muscle cells were resuspended with cell culture medium (DMEM/Ham's F12 1:1) supplemented with 10% fetal calf serum, 2 mM L-glutamine, 2.7 g/l D-glucose, 25 mM HEPES, 100 U/ml penicillin, and 0.1 mg/ml streptomycin, and seeded on glass coverslips for immunofluorescence and single-cell $[Ca^{2+}]_i$ analysis.

For smooth muscle-specific α-actin staining, PASMC were fixed with 4% paraformaldehyde, blocked and permeabilized with PBS including 3% BSA and 0.1% Triton-X100. Coverslips were incubated with monoclonal mouse antibodies against smooth muscle α actin (Sigma

Molecular Pharmacology Fast Forward. Published on October 23, 2015 as DOI: 10.1124/mol.115.100792
This article has not been copyedited and formatted. The final version may differ from this version.

2547; 1:200) overnight. After washing three times for 5 minutes in PBS, alexa fluor 488-conjugated donkey anti-mouse antibody (Invitrogen A21202; 10 µg/ml) was added for 2 hours. Nuclei were stained with Hoechst 33258 (10 µg/ml), coverslips were washed and mounted with Mowiol 4-88 (Roth). All antibodies were diluted and incubated in PBS with 3% BSA. Confocal imaging was performed with a 40x water immersion objective.

To prepare PASMC for Western blotting, cells were harvested with a cell scraper, washed with PBS and homogenized with RIPA buffer, containing 150 mM NaCl, 50 mM Tris, 1 mM EDTA, 1% NP-40, 0.25% natrium deoxycholate, 1 mM NaF, 1 mM natrium orthovanadate, 1 mM PMSF, 1 µg/ml aprotinine, 1 µg/ml leupeptine, and 1 µg/ml pepstatin. After assessment of protein yield using a BCA Protein Assay Kit (Pierce Thermo Scientific, Germany), 30 µg were lysed in Laemmli buffer, and loaded to an 8% SDS-PAGE. Separated proteins were electroblotted onto PVDF membranes, and membranes were blocked for 1 hour in 5% dried milk TBST (20 mM Tris pH 7.4, 137 mM NaCl, 0.1% Tween-20). Anti-TRPC6 antibody (Alomone, Jerusalem; 1:200) or anti β-actin (Sigma; 1:5,000) were incubated in 1% milk TBS, 0.5% Tween-20 overnight. Next day, membrane was washed, followed by incubation with secondary anti-rabbit (TRPC6) or anti-mouse (β-actin) peroxidase-conjugated antibodies (Sigma Aldrich; Germany; 1:5,000) for 3 hours and detection using a chemiluminescence reagent Novex ECL (Invitrogen, Germany).

Molecular Pharmacology Fast Forward. Published on October 23, 2015 as DOI: 10.1124/mol.115.100792
This article has not been copyedited and formatted. The final version may differ from this version.

Smooth muscle cell $[Ca^{2+}]_i$ imaging and Mn^{2+} quench

PASMC were loaded with 5 µM fura-2/AM (Invitrogen) in HBS containing 0.5% BSA for 30 min at 30 min. Coverslips were washed, mounted in a bath chamber and perfused with HBS containing 0.1% BSA. Measurements were performed on an inverted epifluorescence microscope (Carl Zeiss, Jena) equipped with a 10x/0.5 Fluar objective, and a monochromator (Polychrome V, Till Vision) at alternating excitation wavelengths of 340 nm, 358 nm and 380 nm. Digital video imaging was performed with a cooled CCD camera (PCO Sensicam) through a 510-nm long-pass filter. To calibrate Ca^{2+} signals, a spectral unmixing method was used (Lenz et al. 2002). Activation of TRPC6 was induced with 100 µM OAG after a preincubation with 5 µM bisindolylmaleimide (BIM) to exclude PKC interference. To evaluate the activity of store-operated calcium channels (SOC), PASMC were perfused with Ca^{2+}-free HBS and pretreated with 5 µM larixyl acetate or 10 µM lanthanum(III) acetate as positive control. After a stable baseline, 2 µM thapsigargin was injected for 5 min to deplete internal Ca^{2+} stores. Then, 300 µM $MnCl_2$ was added and SOC activity was followed by measuring decreases in fluorescence intensity at 358 nm, corresponding to the isosbestic wavelength of fura-2/AM. In each experiment signals were assessed and averaged from 100-200 cells.

Hypoxia-induced pulmonary vasoconstriction

Acute hypoxia-induced pulmonary vasoconstriction (aHPV) was induced in isolated mouse lungs and assayed as recently described (Urban et al. 2012). In brief, isolated lungs were prepared from male C57BL/6 mice (Charles River Laboratories, St Constant, QC) with a body weight (bw) of 20-30 g and perfused with Hanks' Balanced Salt Solution (HBSS) containing 5% bovine serum albumin and 5% dextran at a rate of 50 mL·kg bw^{-1}·min^{-1}. Pulmonary artery pressure (PAP) was measured continuously during ventilation with a normoxic gas mixture (21% O_2, 5% CO_2, balance N_2) and after switching to hypoxia (1% O_2, 5% CO_2, balance N_2). At both normoxia and hypoxia, flow rates were varied between 25, 50, 75, and 100 mL·kg bw^{-1}·min^{-1} in randomized order for 30 s each to generate a four-point pressure–flow (P-Q) curve from which the intrinsic vascular resistance R_0, i.e. the resistance that would exist if the lung vessels were at their respective diameter at zero vascular pressure, was calculated using a nonlinear regression model (Wang et al. 2012).

Molecular Pharmacology Fast Forward. Published on October 23, 2015 as DOI: 10.1124/mol.115.100792
This article has not been copyedited and formatted. The final version may differ from this version.

Results

Identification of a TRPC6-blocking compound in larch resin

Essential oils, resins, turpentines or balsams of *Pinophyta* (conifers) are frequently applied as homespun remedies to treat or alleviate symptoms of respiratory disorders. To assess a possible TRPC3- and TRPC6-inhibitory activity of oils or resins, we applied several plant extracts, turpentines, resins and essential oils to stably transfected HEK293 cell lines that either overexpress human TRPC6 ($HEK_{TRPC6\text{-}YFP}$) or human TRPC3 ($HEK_{TRPC3\text{-}YFP}$), and measured the effect of serially diluted extracts on the OAG-induced Ca^{2+} responses in a fluorescence imaging plate reader device. Among them, Strasbourg turpentine (silver fir; *Abies alba*), Canada balsam (balsam fir, *Abies balsamea*), Burgundy resin (spruce; *Picea alba*), Pine resin (pine colophony; var. *Pine spp.*), balsam turpentine oil (var. *Pine spp.*), Venice turpentine (a mixture of larch turpentine and colophony), and pure larch turpentine (European larch; *Larix decidua*), or propolis (a resiniferous mixture collected by honey bees) were tested in $HEK_{TRPC6\text{-}YFP}$ or $HEK_{TRPC3\text{-}YFP}$ cells. Both channels were C-terminally tagged with a yellow fluorescent protein to identify clones and later to ascertain the homogeneity of the expression of the respective channel transgene. Fluo-4/AM-loaded $HEK_{hTRPC6\text{-}YFP}$ cell suspensions or adherent cultures of $HEK_{hTRPC3\text{-}YFP}$ cells were incubated with the respective, serially diluted turpentines (dissolved in DMSO) for 5 min, and then challenged with 50 µM OAG to activate Ca^{2+} entry in a receptor- and phospholipase C-independent fashion. As depicted in Figure 1 and Table 1, various conifer turpentines or propolis exerted an inhibitory activity, with Burgundy resin and Strasbourg turpentine having the highest (IC_{50} = 2 mg/l) and lowest (IC_{50} = 200 mg/l) TRPC6-blocking potencies, respectively. At saturating concentrations, the TRPC6 activity was completely abrogated by either coniferous turpentine or resin tested. The preference to block TRPC6, but not TRPC3 was in general poor, with the exception of the larch turpentine. Larch turpentine exerted a relatively high potency (about 13 mg/l) to block the OAG-induced activation of TRPC6, while half-maximal block of TRPC3 was obtained only with about 20-fold higher concentrations of the turpentine (see Fig. 1C, Table 1).

We also asked whether an inhibitory activity is found in essential oils that are frequently inhaled to relieve respiratory symptoms such as cough, bronchospasms or congestion. To test this hypothesis, we applied serial dilutions (20-0.02 ml/l) of the essential oils of various *Pinophyta spp.*, including european larch (*Larix decidua*), and preformed the concentration-

Molecular Pharmacology Fast Forward. Published on October 23, 2015 as DOI: 10.1124/mol.115.100792
This article has not been copyedited and formatted. The final version may differ from this version.

response analysis on $HEK_{hTRPC6\text{-}YFP}$ and $HEK_{hTRPC3\text{-}YFP}$ cells as described for the turpentines (data not shown). None of the conifer oils was capable of blocking TRPC6 at concentrations that are typically used for inhalation, as bathing additives or in ointments. In some cases, the highest concentrations applied in the assay (5-20 ml/l) exerted both increases in $[Ca^{2+}]_I$ and signs of cellular toxicity, such as rounding and swelling of adherent HEK293 cell cultures. Since these signals were unrelated to the expression of the channels, they presumably reflect nonspecific signals. Notably, the TRPC6-prevalent block induced by larch turpentine was not reproduced with the essential oil of *Larix decidua*. We therefore conclude that the biological activity of larch turpentine is contained in its non-volatile resiniferous constituents.

The non-volatile conifer resins contain large amounts of carboxylic acids, such as abietic acid, pimaric acid, or isopimaric acid. When applied individually, these resin acids that are contained in any conifer turpentine were poorly potent and did not exert a marked TRPC6-prevalence in their blocking activity (Fig. 2). When compared to other genus, larch resins contain a fraction of neutral diterpenes that feature a bicyclic, labdane-type structure. The most prominent ones are larixol and larixyl acetate. Larixol exerted a moderate potency (IC_{50} = 2.04 µM) in blocking TRPC6, but showed a marked preference to block TRPC6 compared to TRPC3 (Fig. 3A,C,D). With an IC_{50} of about 0.58 µM, larixyl acetate displayed a higher potency in blocking the OAG-induced Ca^{2+} signals in $HEK_{hTRPC6\text{-}YFP}$ cells (Fig. 3B,C,E). The IC_{50} of 6.38 µM to block TRPC3 demonstrates that the TRPC6-selective activity is maintained in the acetylated derivative. Together, these data suggest that the efficient and selective block of TRPC6 by larixol and larixyl acetate presumably accounts for the TRPC6-selective inhibitory effect of the complete larch turpentine.

Larixol and larixyl acetate-induced inhibition of receptor-induced Ca^{2+} entry through TRPC6

The initial identification of conifer resin constituents as TRPC6-selective inhibitors was achieved by activating TRPC6 or TRPC3 with the membrane-permeable DAG analogue OAG. We next assessed the biological activity of larixol and larixyl acetate to block heterologously expressed TRPC6 channels in a G-protein-coupled receptor (GPCR)-triggered activation regime that includes activation of endogenous phospholipases C in HEK293 cells. The apparent IC_{50} values of larixol and larixyl acetate were 1.57 µM and 0.65 µM when observing the GPCR-induced Ca^{2+} entry in thapsigargin (2 µM for 5 min)-pretreated $HEK_{hTRPC6\text{-}YFP}$ cells (Supplemental Figure 3). Again, the isotype selectivity appeared

Molecular Pharmacology Fast Forward. Published on October 23, 2015 as DOI: 10.1124/mol.115.100792
This article has not been copyedited and formatted. The final version may differ from this version.

considerably high, since GPCR-induced activation of Ca^{2+} entry through TRPC3 was half maximally inhibited by 19.0 ± 0.9 µM larixol or by 7.3 ± 0.7 µM larixyl acetate (data not shown). Thus, the about 12-fold preference of larixyl acetate to block TRPC6 compared to TRPC3 in the OAG-activated mode was confirmed by an about 11-fold higher potency of the compound in the GPCR-activated mode of TRPC6 and TRPC3.

Larixyl acetate does not interfere with GPCR-induced phospholipase C activation

To exclude that the most potent TRPC6 blocker larixyl acetate uncouples the GPCR-induced activation of phospholipase C, we measured the Ca^{2+} mobilisation response by stimulating parental HEK293 cells in a Ca^{2+}-free HBS (1 mM Ca^{2+} replaced by 200 µM EGTA, pH 7.4) with 300 µM ATP, 1 mM carbachol or 0.5 U/ml thrombin without thapsigargin pretreatment. The resulting transient increases in $[Ca^{2+}]_i$ were essentially identical irrespective of the presence or absence of 10 µM larixyl acetate, a concentration which blocks TRPC6 activity by more than 90% (Fig. 4A,B). The PLC-mediated formation of endogenous DAG species and possible effects on DAG availability or degradation were more directly assessed by monitoring the plasma membrane recruitment of a fluorescent fusion protein of the C1 domain-bearing protein kinase Cε (PKCε-YFP) upon receptor activation in the absence and in the presence of 10 µM larixyl acetate. Applying confocal life cell microscopy, the plasma membrane association can be quantified by following the background-corrected fluorescence intensity of PKCε-YFP in the cytosol before ($I_{cyt}(0)$) and during ($I_{cyt}(t)$) GPCR activation. Since PKCε-YFP is not enriched in the plasma membrane of resting cells, and since PKCε-YFP is selectively recruited to the plasma membrane (Fig. 4C), the fraction of plasma membrane-bound PKCε is reflected by the fluorescence disappearance in the cytosol by calculating $I_{PM}(t) = (I_{cyt}(0\ s) - I_{cyt}(t)) / I_{cyt}(0\ s)$. The results showed that 10 µM larixyl acetate did not cause a significant decrease in the GPCR-triggered translocation efficiency of PKCε-YFP (Fig. 4D,E). We conclude that larixyl acetate does not interfere with the GPCR-induced activation of phospholipase C or accelerates DAG breakdown, but presumably acts by direct TRPC6 channel inhibition.

Isoform selectivity of TRP channel block by larch-derived labdanes

The selectivity of the identified TRPC6 inhibitors was further profiled with TRPC7, and with TRPC4 and TRPC5, representing the more distantly related TRPC family members. In line

Molecular Pharmacology Fast Forward. Published on October 23, 2015 as DOI: 10.1124/mol.115.100792
This article has not been copyedited and formatted. The final version may differ from this version.

with the phylogenetic distance, OAG-activated TRPC7 was inhibited with an IC_{50} of 2.9 μM, whereas half-maximal block of GPCR-induced activation of TRPC4β and TRPC5 required 18.0 and 19.3 μM concentrations of the compound, respectively (Fig. 5A). Of note, a steeper concentration response curve was seen for TRPC7. This effect may be caused by a distinct and more cooperative mode of inhibition or by changes of the channel inactivation properties. Extending the range of TRP channels to TRPV1, TRPV4, TRPM2, and TRPM8 revealed no discernible inhibition at 15 μM concentrations that almost completely block TRPC6 (Fig. 5B). In FLIPR analyses, TRPM3 was weakly inhibited by 15 μM larixyl acetate, but no statistically significant inhibition was seen in single-cell $[Ca^{2+}]_i$ analyses, or in electrophysiological experiments when acutely applying up to 15 μM larixyl acetate (data not shown).

To assess the activity of larixyl acetate on the $Ca_V1.2$ subtype of voltage-gated Ca^{2+} channels, heterologously expressed $Ca_V1.2$ was analysed electrophysiologically by applying voltage step protocols. Robust $Ca_V1.2$ currents were obtained by stepping the membrane potential from -70 mV to +20 mV (Supplemental Figure 4). In contrast to 1 μM nifedipine, 5-10 μM larixyl acetate exerted only a partial and statistically not significant inhibition of $Ca_V1.2$-mediated peak current densities. Similarly, the inactivation time constants remained unchanged in the presence of 5 μM or 10 μM larixyl acetate.

Although rat pulmonary artery smooth muscle cells almost exclusively expressed TRPC6, but not TRPC3, these channel subunits may be co-expressed in vascular smooth muscle cells of other tissues and species. To assess the impact of larixyl acetate in cells that are assumed to form heteromeric TRPC6:TRPC3 channel complexes, we generated a stable $HEK_{TRPC6:YFP:TRPC3:CFP}$ cell line, which co-express both channel subunits. The stoichiometry of TRPC6:TRPC3 expression was estimated by comparing CFP and YFP fluorescence intensities to those in cells which expressed an intramolecularly fused CFP-YFP fusion protein, with CFP intensities detected after eliminating Förster resonance energy transfer (FRET) by photobleaching YFP. The stable cell line expresses TRPC6-YFP and TRPC3-CFP at a 1:2 ratio (Fig. 5C). As reported earlier, TRPC6 channel assembly can be monitored by FRET assays (Hofmann et al. 2002). In $HEK_{TRPC6:YFP:TRPC3:CFP}$ cells subjected to the method described therein, the FRET efficiency was about 35% lower than in transiently transfected HEK293 cells, expressing both subunits at a 1:1 stoichiometry (see Fig. 5C). The slight reduction of FRET efficiencies in the stable cell line expressing the partners with a molar excess of the FRET donor (TRPC3-CFP) is in good agreement with a maintained

Molecular Pharmacology Fast Forward. Published on October 23, 2015 as DOI: 10.1124/mol.115.100792
This article has not been copyedited and formatted. The final version may differ from this version.

heteromer formation, but a fraction of homomeric TRPC3-CFP and a lower abundance of FRET acceptors (TRPC6-YFP) in individual channel complexes. Assuming a channel subunit assembly with no preference for momomeric versus heteromeric association, the expected percentage of homomeric TRPC3 and homomeric TRPC6 channels in this cell line amounts 19.2% and 1.3%, respectively. Hence, most TRPC6-YFP channel subunits would be contained in heteromeric complexes along with one (10.2%), two (30.0%) or three (39.2%) TRPC3-CFP subunits. In these cells, larixyl acetate inhibited the OAG-induced $[Ca^{2+}]_i$ signal with an IC_{50} of about 3.74 μM (Fig. 5D), hinting to a TRPC6 homomer-prevalent inhibitory property of larixyl acetate.

Electrophysiological characterisation of the TRPC6 block

The electrophysiological properties of larixyl acetate were determined in HEK293 cells that stably expressed TRPC6 ($HEK_{hTRPC6\text{-}YFP}$) or TRPC3 ($HEK_{hTRPC3\text{-}YFP}$). In $HEK_{hTRPC6\text{-}YFP}$ cells, stimulation with 50 μM OAG elicited a characteristic non-selective cation conductance with a reversal potential close to 0 mV and a dually rectifying current-voltage relationship. In the presence of 0.1-5 μM larixyl acetate, inward and outward currents through TRPC6 were concentration-dependently blocked (Fig. 6A-C). Of note, the half-maximally inhibitory concentrations of larixyl acetate to block TRPC6 inward and outward currents were 0.12-0.13 μM (Fig. 6E), which is markedly lower than the concentrations that were required to half-maximally suppress increases in fluo-4 fluorescence. In agreement with the selectivity observed in $[Ca^{2+}]_i$ assays, TRPC3 current inhibition required substantial higher larixyl acetate concentrations with half-maximal effects seen at concentrations of 1.4 μM (Fig. 6D,F). The analysis of current-voltage relationships in I/V curves provided no evidence for a voltage-dependence of the TRPC6 block (see Fig. 6B). It should, however, be mentioned that, upon addition of larixyl acetate, the physiologically relevant inward currents (at -100 mV) decayed slightly faster than outward currents measured at +100 mV. Since both TRPC6 channel opening and channel inactivation/closure typically develop in a voltage-dependent fashion with outward currents preceding the development and lagging behind the decay of inward currents, this partially voltage-sensitive behaviour of the blocker is not unexpected.

To assess the reversibility of the inhibition, intracellularly perfused fluoroaluminate was used to obtain a persistent G protein activation and more long-lasting TRPC6 currents. Inhibition by 1 μM larixyl acetate was again effective, and the block was reversible upon wash-out of

Molecular Pharmacology Fast Forward. Published on October 23, 2015 as DOI: 10.1124/mol.115.100792
This article has not been copyedited and formatted. The final version may differ from this version.

the compound (Fig. 7A,B). A second addition of the blockers was again effective, indicating a slowly developing, but fully reversible and repeatable mode of action (Fig. 7C,D). Of note, larixyl acetate added to the pipette solution that was used for recordings in the whole cell mode, did not prevent the activation of TRPC6 by intracellularly perfused fluoroaluminate or by extracellularly applied OAG (grey trace and bars in Fig. 7A,B). Under these conditions, TRPC6 activation was still blocked by adding larixyl acetate to the bath solution. To further substantiate the observation that larixyl acetate preferentially gets access to its binding site from the extracellular side, we compared the effectiveness of bath solution-applied larixyl acetate in excised inside-out and outside-out membrane patches. Indeed, TRPC6 currents inside-out patches were less efficiently inhibited by 1 μM larixyl acetate (Fig. 7E,F) than those measured in the outside-out configuration (Fig. 7G,H). Owing to the very short (< 1 ms) mean open time of TRPC6, the kinetics of the block is hardly resolvable, using electrophysiological patch clamp methods. Since single channel openings in the presence of larixyl acetate appear less frequent, but can still reach amplitudes of more than 4 pA (see insets in Fig. 7E,G), a slow or flickery mode of channel inhibition is assumed.

Assessment of cytotoxic activity and of stability in human blood

The application of pharmacological TRPC6 modulators in more complex systems *ex vivo* or *in vivo* requires the absence of cytotoxic effects of the respective modulator. To follow possible acute and subacute cytotoxic effects of larixol or larixyl acetate, we tested the membrane integrity upon 10 min or 24 h exposure of HEK293 cells to various compound concentrations with a propidium iodide assay. Under these conditions, no discernible membrane instability was elicited by larixol or larixyl acetate (Fig. 8A,B). Likewise, cellular viability and proliferation appeared unaffected by both compounds as tested with a colorimetric MTT (3-(4,5-dimethylthiazol-2-yl)-2,5-diphenyltetrazolium bromide) conversion test (Fig. 8C). To gain first insight into the stability of larixyl acetate in human blood samples, the compound was added to citrate-supplemented whole-blood samples for up to 24 h, and the remaining bioactivity was tested in $HEK_{hTRPC6\text{-}YFP}$ cells by applying an appropriate dilution of cleared supernatants, containing an initial concentration of 10 μM larixyl acetate. The block of TRPC6 activity was not impaired by prolonged exposure to human blood obtained from three different donors (see Fig. 8D).

Molecular Pharmacology Fast Forward. Published on October 23, 2015 as DOI: 10.1124/mol.115.100792
This article has not been copyedited and formatted. The final version may differ from this version.

Biological activity of larixyl acetate to block native TRPC6-like channels

TRPC6 is expressed in pulmonary artery smooth muscle (PASM) cells. In primary cultures of rat PASM, TRPC6 expression was confirmed by Western blot analysis, and immunofluorescence detection of smooth muscle-specific α-actin confirmed the purity of PASM cell cultures and ongoing expression of contractile filaments (Fig. 9A). In these cells, TRPC6-like responses were elicited by stimulation with OAG (100 µM), which caused a significant rise of the intracellular Ca^{2+} concentrations in about 70-100% of PASM cells, reaching an average peak concentration of about 300 nM $[Ca^{2+}]_i$ (Fig. B). The acute addition of 5 µM larixyl acetate resulted in a rapid decline of $[Ca^{2+}]_i$ (see grey line in Fig. 9B) compared to the untreated controls. Upon preincubation with 1 µM or 5 µM larixyl acetate, the OAG-stimulated increase in $[Ca^{2+}]_i$ was strongly or completely suppressed (see Fig. 9C,D), indicating an efficient inhibition of native TRPC6 channel complexes. Inclusion of 5 µM bisindolylmaleimide 1 (BIM) served to ascertain that these effects are independent of protein kinase C activation by OAG. By contrast, the store-depletion-associated Mn^{2+} entry in thapsigargin-treated PASM cells was unaffected by 5 µM larixyl acetate, but completely abrogated by 10 µM La^{3+} (Fig. 9E,F). Electrophysiological recordings of OAG-stimulated whole-cell currents in PASM cells revealed TRPC6-like transient inward and outward currents, reversing close to 0 mV and showing the typical “n”-shaped current-voltage relationship (Fig. 10). Acute addition of 5 µM larixyl acetate at a time point close to the maximal activation levels led to an immediate decay of both outward and inward currents (Fig. 10B). Together, these data strongly suggest a reliable block of TRPC6-like channels but not store-operated channels by the larixol derivative in rat PASM cells.

Larixyl acetate prevents the hypoxia-induced pulmonary vasoconstriction

To test the impact of larixyl acetate on a physiologically relevant response that involves TRPC6 activation, we measured the hypoxia-induced pulmonary vasoconstriction (HPV), also referred to as the “von Euler-Lilljestrand mechanism”. In the isolated mouse lung, a perfusion pressure of 5.7 ± 0.3 mmHg was required to achieve and maintain a baseline flow rate of 50 mL·kg bw^{-1}·min^{-1} during normoxic ventilation. After switching to hypoxic ventilation the perfusion pressure increased by 2.5 ± 0.2 mmHg, reaching peak values about 10 min after the onset of hypoxic ventilation. In the presence of 5 µM larixyl acetate applied via the

Molecular Pharmacology Fast Forward. Published on October 23, 2015 as DOI: 10.1124/mol.115.100792
This article has not been copyedited and formatted. The final version may differ from this version.

perfusate, the increase in the perfusion pressure upon hypoxic ventilation was suppressed by 80% ($p = 0.008$; $n = 5$; Fig. 11A,B).

Before and 10 min after switching to hypoxic ventilation, the vascular resistance was determined by applying a discontinuous flow ramp (25-100 ml min^{-1} kg^{-1}) and calculating the intrinsic vascular resistance R_0. R_0 increased from 0.25 ± 0.03 to 0.53 ± 0.13 $mmHg \cdot mL^{-1} \cdot kg\ bw^{-1} \cdot min^{-1}$ during hypoxic ventilation, yet this effect was strongly attenuated in mouse lungs that were perfused with 5 μM larixyl acetate (Fig. 11C).

Molecular Pharmacology Fast Forward. Published on October 23, 2015 as DOI: 10.1124/mol.115.100792
This article has not been copyedited and formatted. The final version may differ from this version.

Discussion

In this study, larch-derived diterpenes have been identified as a new class of natural compounds that exhibit TRPC6-inhibitory biological activity. In contrast to the recently reported subfamily-spanning inhibitor norgestimate (Miehe et al. 2012) or a slightly more TRPC6-selective inhibitor 8009-5364 (Urban et al. 2012), larixol and larixyl acetate display a marked selectivity for a single isotype of the closely related TRPC3/6/7 subfamily. Since electrophysiological analyses directly monitor the channel activity, the estimated IC_{50} of larixyl acetate to block inward currents through TRPC6 is about 0.1 µM. The selectivity of TRPC6 inhibition compared to TRPC3 is about 12-fold. Thus, together with the recently disclosed compound SAR7334, a substituted aminoindanole that also displays an about 20- to 30-fold selectivity for TRPC6 over TRPC3 or TRPC7 (Maier et al. 2015), larixyl acetate can be considered a TRPC6-selective blocker. The inhibition of TRPC6 activity is reversible, largely voltage-independent and affects both Ca^{2+} and Na^{+} entry through TRPC6, while leaving the GPCR-induced activation of phospholipase C and protein kinase C translocation unaffected. Similar to the recombinantly expressed human TRPC6, native TRPC6-related Ca^{2+} entry in rat pulmonary artery smooth muscle cells was efficiently suppressed by low micromolar concentrations of larixyl acetate. Low cytotoxicity of the compound allowed the application of the inhibitor in an *ex vivo* model of hypoxia-induced pulmonary vasoconstriction in mouse lungs, mimicking the effect of TRPC6 deficiency to abrogate the early vasoconstrictive response to hypoxia known as the von Euler-Liljestrand mechanism.

Previous publications highlighted a prominent interaction of various natural compounds with TRP channels to activate, positively modulate, or inhibit the channel activity. Our initial finding that conifer turpentines contain TRPC6- and TRPC3-inhibitory activity was a starting point for further screening of different conifer species and extracts. Since the turpentine of *Larix decidua* (European larch) displayed a noticeable TRPC6-prevalent biological activity, we focused our interest on identifying its active ingredient. Larch turpentine consists of 15% (w/w) essential oils that were not acting as TRPC6 inhibitors. The non-distillable resin contains resin acids that are common for various Pinaceae and displayed inhibitory activity towards both TRPC6 and TRPC3. In the genus *Larix*, the neutral fraction contains substantial amounts of larixyl acetate (Sandermann et al. 1965). By testing subfractions and, finally, the larch-specific resin components larixol and larixyl acetate, the selective inhibitory activity was

Molecular Pharmacology Fast Forward. Published on October 23, 2015 as DOI: 10.1124/mol.115.100792
This article has not been copyedited and formatted. The final version may differ from this version.

identified in the two chemically defined compounds. In contrast to the biological activity of some monoterpenes on cation channels, including TRP channels (Oz et al. 2015), a channel-modulating activity of larch-derived bicyclic diterpenes has not yet been described. A calcium channel inhibition by other labdane diterpenes has been occasionally reported (de Oliveira et al. 2006; El-Bardai et al. 2003), but the inhibition of $Ca_V1.2$ currents required concentrations that are more than two orders of magnitude higher than the inhibitory activity of larixyl acetate towards TRPC6 currents. Thus, to our knowledge, there is no evidence for a promiscuous activity of larixyl acetate or other labdane- or labdene-type diterpenes to potently inhibit Ca^{2+}-permeable ion channels or affect other modulators of cellular Ca^{2+} homeostasis.

Until the end of the 20th century, Venetian turpentine, a mixture of larch turpentine and pine resin (colophony), was available in pharmacy and externally applied for wound disinfection. In addition, larch resin was slowly burned, and vapors were inhaled for relaxation and invigoration of respiratory organs. The larch resin was also used as a gum by Native Americans, and in Siberia to treat toothaches. Larch sawdust, a cheap byproduct of wood industry, has been proposed as feed supplement for pigs and ruminants with anti-inflammatory activity (Bauer et al. 2009). In vitro, labdane-type diterpenes have been implicated with inhibition of COX-2 and leukotriene LTB4 formation (Pferschy-Wenzig et al. 2008). The European Medical Agency lists larch turpentine as *Terebinthinae laricina* for topical application as an antiseptic and wound healing-promoting drug in veterinary medicinal products (EMEA/MRL/398/98). Likewise, larch turpentine is contained in some commercially available balsams and ointments.

Orally ingested conifer turpentine has been reported to exert acute toxicity with an LD_{50} of 5760 mg/kg in rats (Skramlik 1959). The highly lipophilic and volatile essential oils of conifer trees, such as pinenes and other bicyclic monoterpenes may cause toxicity upon inhalation, cutaneous exposure or massive oral ingestion (Mercier et al. 2009). By contrast, the toxicity of the resiniferous ingredients in larch turpentines, including larixol or larixyl acetate is not reported in detail. To gain first insight into cytotoxicity and a possible interference with cell proliferation in the presence of larixol and larixyl acetate, we performed a propidium iodide staining and a MTT assay in HEK293 cells. Only a prolonged incubation with high

Molecular Pharmacology Fast Forward. Published on October 23, 2015 as DOI: 10.1124/mol.115.100792
This article has not been copyedited and formatted. The final version may differ from this version.

micromolar concentrations of larixyl acetate exerted a marked reduction of metabolic activity, indicative of a cytotoxic effect.

The biological activity of larixyl acetate on native, TRPC6-like signals in PASM cells, and in abrogating acute HPV in mouse lungs suggests that the compound is effective on native, TRPC6-bearing ion channel complexes. The complex signalling mechanism behind HPV is not yet fully elucidated, but the available data suggest that several intermediates are critical. Besides TRPC6, other ion channels have been implicated in mediating HPV, including TRPV4 (Goldenberg et al. 2015), voltage-gated potassium channels and, obviously, voltage-gated calcium channels in vascular smooth muscle cells (Veit et al. 2015). Therefore, selectivity tests were extended to cover the Ca^{2+}-permeable TRPV4 and $CaV_{1.2}$. Although these channels are not (TRPV4) or only poorly inhibited by larixyl acetate ($CaV_{1.2}$), we cannot exclude that other ion channels or non-channel targets may contribute to the inhibition of HPV observed in isolated mouse lungs.

Owing to the ester bond, the stability of the natural compound may be compromised by unspecific serum esterases. Since the activity was maintained upon prolonged incubation in whole blood, the acetate ester seems to withstand these plasma esterases. At present, however, the pharmacokinetic properties of larixyl acetate, including oral bioavailability, distribution volume, metabolism and elimination half times are not yet known. Thus, long-term treatments, for example to prevent or delay the progression of TRPC6-related kidney diseases in preclinical disease models, will require characterisation of the absorption, distribution, metabolism, and excretion (ADME) profile of larixyl acetate. Since larixol is readily available in gram amounts, further compound optimisation within the chemical entity may be promising. Other applications, such as protection from pulmonary vasoconstriction, bronchoconstriction, and allergic airway disease, may be realised via nebulizer-assisted topic application, thereby circumventing uncertainties of hepatic first-pass metabolism and lowering the systemic exposure to the drug.

Although the process of validating TRPC6 as a potential pharmacological target is still ongoing, specific pulmonary and renal diseases are the most advanced examples in which TRPC6 inhibition may resolve currently unmet medical needs. In the lung, dysregulated

Molecular Pharmacology Fast Forward. Published on October 23, 2015 as DOI: 10.1124/mol.115.100792
This article has not been copyedited and formatted. The final version may differ from this version.

TRPC6 activity may contribute to pulmonary hypertension (Smith et al. 2015; Yu et al. 2009), allergic airway disease (Sel et al. 2008), and ischemia-reperfusion associated oedema (Weissmann et al. 2012) or permeability-type barrier failure (Samapati et al. 2012). In the kidney, familial forms of focal segmental glomerulosclerosis are a prominent phenotype that can be caused by gain-of-function mutations in the TRPC6 gene or by TRPC6 overexpression (Krall et al. 2010; Winn et al. 2005). On the other hand, TRPC6 seems to protect podocytes from complement-induced injury (Kistler et al. 2013). Hence, further work is required for dissecting out potential fields of use for pharmacological modulators of TRPC6. Of note, the marked TRPC6 expression in the dentate gyrus of the hippocampus (Nagy et al. 2013), contributing to the regulation of neurite outgrowth (Heiser et al. 2013), may either give rise to additional fields of use or - if inhibition would be detrimental - pose a need to avoid blood-brain-barrier permeability of pharmacological TRPC6 modulators. In addition, the acute modulation of TRPC6 may circumvent problems that can arise from a compensatory upregulation of other TRPC channels, an effect that has been observed in vascular smooth muscle cells of TRPC6-deficient animals (Dietrich et al. 2005). Therefore, the development of selectively acting pharmacological TRPC6 inhibitors is expected to fuel future studies that contribute to a more precise understanding of physiological and pathophysiological functions of this member of the TRP channel family.

Molecular Pharmacology Fast Forward. Published on October 23, 2015 as DOI: 10.1124/mol.115.100792
This article has not been copyedited and formatted. The final version may differ from this version.

Acknowledgments

This work was supported by the Deutsche Forschungsgemeinschaft (TRR 152).

Authorship Contributions

Participated in research design: Rademann, Kuebler, Schaefer.

Conducted experiments: Urban, Wang, Kwiek.

Contributed new reagents or analytic tools: Kwiek, Rademann.

Performed data analysis: Urban, Kuebler, Schaefer.

Wrote or contributed to the writing of the manuscript: Urban, Kuebler, Schaefer.

Molecular Pharmacology Fast Forward. Published on October 23, 2015 as DOI: 10.1124/mol.115.100792
This article has not been copyedited and formatted. The final version may differ from this version.

References

Bauer R, Wenzig E-M, Franz C, Stefanon B, Tzika E, Kyriakis S, Farinacci M, and Sgorlon S (2009) Use larch wood material for treating inflammation. *WO 2009079680 A1.*

de Oliveira AP, Furtado FF, da Silva MS, Tavares JF, Mafra RA, Araujo DA, Cruz JS, and de Medeiros IA (2006) Calcium channel blockade as a target for the cardiovascular effects induced by the 8(17),12E,14-labdatrien-18-oic acid (labdane-302). *Vascul Pharmacol* **44**:338-344.

Dietrich A, Chubanov V, Kalwa H, Rost BR, and Gudermann T (2006) Cation channels of the transient receptor potential superfamily: their role in physiological and pathophysiological processes of smooth muscle cells. *Pharmacol Ther* **112**:744-760.

Dietrich A, Mederos YS, Gollasch M, Gross V, Storch U, Dubrovska G, Obst M, Yildirim E, Salanova B, Kalwa H, Essin K, Pinkenburg O, Luft FC, Gudermann T, and Birnbaumer L (2005) Increased vascular smooth muscle contractility in TRPC6$^{-/-}$ mice. *Mol Cell Biol* **25**:6980-6989.

El-Bardai S, Wibo M, Hamaide MC, Lyoussi B, Quetin-Leclercq J, and Morel N (2003) Characterisation of marrubenol, a diterpene extracted from Marrubium vulgare, as an L-type calcium channel blocker. *Br J Pharmacol* **140**:1211-1216.

Finney-Hayward TK, Popa MO, Bahra P, Li S, Poll CT, Gosling M, Nicholson AG, Russell RE, Kon OM, Jarai G, Westwick J, Barnes PJ, and Donnelly LE (2010) Expression of transient receptor potential C6 channels in human lung macrophages. *Am J Respir Cell Mol Biol* **43**:296-304.

Fuchs B, Rupp M, Ghofrani HA, Schermuly RT, Seeger W, Grimminger F, Gudermann T, Dietrich A, and Weissmann N (2011) Diacylglycerol regulates acute hypoxic pulmonary vasoconstriction via TRPC6. *Respir Res* **12**:20.

Goldenberg NM, Wang L, Ranke H, Liedtke W, Tabuchi A, and Kuebler WM (2015) TRPV4 is required for hypoxic pulmonary vasoconstriction. *Anesthesiology* **122**:1338-1348.

Gudermann T, Hofmann T, Schnitzler M, and Dietrich A (2004) Activation, subunit composition and physiological relevance of DAG-sensitive TRPC proteins. *Novartis Found Symp* **258**:103-118.

Heiser JH, Schuwald AM, Sillani G, Ye L, Muller WE, and Leuner K (2013) TRPC6 channel-mediated neurite outgrowth in PC12 cells and hippocampal neurons involves activation of RAS/MEK/ERK, PI3K, and CAMKIV signaling. *J Neurochem* **127**:303-313.

Hofmann T, Obukhov AG, Schaefer M, Harteneck C, Gudermann T, and Schultz G (1999) Direct activation of human TRPC6 and TRPC3 channels by diacylglycerol. *Nature* **397**:259-263.

Hofmann T, Schaefer M, Schultz G, and Gudermann T (2002) Subunit composition of mammalian transient receptor potential channels in living cells. *Proc Natl Acad Sci U S A* **99**:7461-7466.

Kistler AD, Singh G, Altintas MM, Yu H, Fernandez IC, Gu C, Wilson C, Srivastava SK, Dietrich A, Walz K, Kerjaschki D, Ruiz P, Dryer S, Sever S, Dinda AK, Faul C, and Reiser J (2013) Transient receptor potential channel 6 (TRPC6) protects podocytes during complement-mediated glomerular disease. *J Biol Chem* **288**:36598-36609.

Krall P, Canales CP, Kairath P, Carmona-Mora P, Molina J, Carpio JD, Ruiz P, Mezzano SA, Li J, Wei C, Reiser J, Young JI, and Walz K (2010) Podocyte-specific overexpression of wild type or mutant trpc6 in mice is sufficient to cause glomerular disease. *PLoS One* **5**:e12859.

Lenz JC, Reusch HP, Albrecht N, Schultz G, and Schaefer M (2002) Ca^{2+}-controlled competitive diacylglycerol binding of protein kinase C isoenzymes in living cells. *J Cell Biol* **159**:291-302.

Maier T, Follmann M, Hessler G, Kleemann HW, Hachtel S, Fuchs B, Weissmann N, Linz W, Schmidt T, Lohn M, Schroeter K, Wang L, Rutten H, and Strübing C (2015) Discovery and pharmacological characterization of a novel potent inhibitor of diacylglycerol-sensitive TRPC cation channels. *Br J Pharmacol* **172**:3650-3660.

Mercier B, Prost J, and Prost M (2009) The essential oil of turpentine and its major volatile fraction (alpha- and beta-pinenes): a review. *Int J Occup Med Environ Health* **22**:331-342.

Miehe S, Crause P, Schmidt T, Lohn M, Kleemann HW, Licher T, Dittrich W, Rutten H, and Strübing C (2012) Inhibition of diacylglycerol-sensitive TRPC channels by synthetic and natural steroids. *PLoS One* **7**:e35393

Nagy GA, Botond G, Borhegyi Z, Plummer NW, Freund TF, and Hajos N (2013) DAG-sensitive and Ca^{2+} permeable TRPC6 channels are expressed in dentate granule cells and interneurons in the hippocampal formation. *Hippocampus* **23**:221-232.

Okada T, Inoue R, Yamazaki K, Maeda A, Kurosaki T, Yamakuni T, Tanaka I, Shimizu S, Ikenaka K, Imoto K, and Mori Y (1999) Molecular and functional characterization of a novel mouse transient receptor potential protein homologue TRP7. *J Biol Chem* **274**:27359-27370.

Ong HL, De Souza LB, Cheng KT, and Ambudkar IS (2014) Physiological functions and regulation of TRPC channels. *Handb Exp Pharmacol* **223**:1005-1034.

Oz M, Lozon Y, Sultan A, Yang KH, and Galadari S (2015) Effects of monoterpenes on ion channels of excitable cells. *Pharmacol Ther* **152**:83-97.

Pferschy-Wenzig EM, Kunert O, Presser A, and Bauer R (2008) In vitro anti-inflammatory activity of larch (*Larix decidua L.*) sawdust. *J Agric Food Chem* **56**:11688-11693.

Reiser J, Polu KR, Moller CC, Kenlan P, Altintas MM, Wei C, Faul C, Herbert S, Villegas I, Avila-Casado C, McGee M, Sugimoto H, Brown D, Kalluri R, Mundel P, Smith PL, Clapham DE, and Pollak MR (2005) TRPC6 is a glomerular slit diaphragm-associated channel required for normal renal function. *Nat Genet* **37**:739-744.

Romanin C, Gamsjaeger R, Kahr H, Schaufler D, Carlson O, Abernethy DR, and Soldatov NM (2000) Ca^{2+} sensors of L-type Ca^{2+} channel. *FEBS Lett* **487**:301-306.

Samapati R, Yang Y, Yin J, Stoerger C, Arenz C, Dietrich A, Gudermann T, Adam D, Wu S, Freichel M, Flockerzi V, Uhlig S, and Kuebler WM (2012) Lung endothelial Ca^{2+} and permeability response to platelet-activating factor is mediated by acid sphingomyelinase and transient receptor potential classical 6. *Am J Respir Crit Care Med* **185**:160-170.

Sandermann W and Bruns K (1965) Über die Konformation des Larixols. *Tetrahedon Letters* **42**:3757-3760.

Schaefer M, Albrecht N, Hofmann T, Gudermann T, and Schultz G (2001) Diffusion-limited translocation mechanism of protein kinase C isotypes. *FASEB J* **15**:1634-1636.

Sel S, Rost BR, Yildirim AO, Sel B, Kalwa H, Fehrenbach H, Renz H, Gudermann T, and Dietrich A (2008) Loss of classical transient receptor potential 6 channel reduces allergic airway response. *Clin Exp Allergy* **38**:1548-1558.

Skramlik EV (1959) Über die Giftigkeit und Verträglichkeit von ätherischen Ölen. *Pharmazie* **14**:435-445.

Smith KA, Voiriot G, Tang H, Fraidenburg DR, Song S, Yamamura H, Yamamura A, Guo Q, Wan J, Pohl NM, Tauseef M, Bodmer R, Ocorr K, Thistlethwaite PA, Haddad GG, Powell FL, Makino A, Mehta D, and Yuan JX (2015) Notch activation of Ca^{2+} signaling mediates hypoxic pulmonary vasoconstriction and pulmonary hypertension. *Am J Respir Cell Mol Biol* **53**:355-367.

Tabeling C, Yu H, Wang L, Ranke H, Goldenberg NM, Zabini D, Noe E, Krauszman A, Gutbier B, Yin J, Schaefer M, Arenz C, Hocke AC, Suttorp N, Proia RL, Witzenrath M, and Kuebler WM (2015) CFTR and sphingolipids mediate hypoxic pulmonary vasoconstriction. *Proc Natl Acad Sci U S A* **112**:E1614-E1623.

Urban N, Hill K, Wang L, Kuebler WM, and Schaefer M (2012) Novel pharmacological TRPC inhibitors block hypoxia-induced vasoconstriction. *Cell Calcium* **51**:194-206.

Veit F, Pak O, Brandes RP, and Weissmann N (2015) Hypoxia-dependent reactive oxygen species signaling in the pulmonary circulation: focus on ion channels. *Antioxid Redox Signal* **22**:537-552.

Wang L, Yin J, Nickles HT, Ranke H, Tabuchi A, Hoffmann J, Tabeling C, Barbosa-Sicard E, Chanson M, Kwak BR, Shin HS, Wu S, Isakson BE, Witzenrath M, de WC, Fleming I, Kuppe H, and Kuebler WM (2012) Hypoxic pulmonary vasoconstriction requires connexin 40-mediated endothelial signal conduction. *J Clin Invest* **122**:4218-4230.

Wang YX and Zheng YM (2011) Molecular expression and functional role of canonical transient receptor potential channels in airway smooth muscle cells. *Adv Exp Med Biol* **704**:731-747.

Weissmann N, Dietrich A, Fuchs B, Kalwa H, Ay M, Dumitrascu R, Olschewski A, Storch U, Schnitzler M, Ghofrani HA, Schermuly RT, Pinkenburg O, Seeger W, Grimminger F, and Gudermann T (2006) Classical transient receptor potential channel 6 (TRPC6) is essential for hypoxic pulmonary vasoconstriction and alveolar gas exchange. *Proc Natl Acad Sci U S A* **103**:19093-19098.

Weissmann N, Sydykov A, Kalwa H, Storch U, Fuchs B, Schnitzler M, Brandes RP, Grimminger F, Meissner M, Freichel M, Offermanns S, Veit F, Pak O, Krause KH, Schermuly RT, Brewer AC, Schmidt HH, Seeger W, Shah AM, Gudermann T, Ghofrani HA, and Dietrich A (2012) Activation of TRPC6 channels is essential for lung ischaemia-reperfusion induced oedema in mice. *Nat Commun* **3**:649-649.

Welsh DG, Morielli AD, Nelson MT, and Brayden JE (2002) Transient receptor potential channels regulate myogenic tone of resistance arteries. *Circ Res* **90**:248-250.

Winn MP, Conlon PJ, Lynn KL, Farrington MK, Creazzo T, Hawkins AF, Daskalakis N, Kwan SY, Ebersviller S, Burchette JL, Pericak-Vance MA, Howell DN, Vance JM, and Rosenberg PB (2005) A mutation in the TRPC6 cation channel causes familial focal segmental glomerulosclerosis. *Science* **308**:1801-1804.

Molecular Pharmacology Fast Forward. Published on October 23, 2015 as DOI: 10.1124/mol.115.100792
This article has not been copyedited and formatted. The final version may differ from this version.

Yu Y, Fantozzi I, Remillard CV, Landsberg JW, Kunichika N, Platoshyn O, Tigno DD, Thistlethwaite PA, Rubin LJ, and Yuan JX (2004) Enhanced expression of transient receptor potential channels in idiopathic pulmonary arterial hypertension. *Proc Natl Acad Sci U S A* **101**:13861-13866.

Yu Y, Keller SH, Remillard CV, Safrina O, Nicholson A, Zhang SL, Jiang W, Vangala N, Landsberg JW, Wang JY, Thistlethwaite PA, Channick RN, Robbins IM, Loyd JE, Ghofrani HA, Grimminger F, Schermuly RT, Cahalan MD, Rubin LJ, and Yuan JX (2009) A functional single-nucleotide polymorphism in the TRPC6 gene promoter associated with idiopathic pulmonary arterial hypertension. *Circulation* **119**:2313-2322.

Molecular Pharmacology Fast Forward. Published on October 23, 2015 as DOI: 10.1124/mol.115.100792
This article has not been copyedited and formatted. The final version may differ from this version.

Legends for Figures

Figure 1: Conifer turpentines or resins concentration-dependently block Ca^{2+} entry through TRPC6 and TRPC3.

HEK293 cell lines that stably express TRPC6 ($HEK_{hTRPC6\text{-}YFP}$; black symbols and lines) or TRPC3 ($HEK_{hTRPC3\text{-}YFP}$; grey symbols and lines) were loaded with fluo-4/AM in suspension and dispensed (TRPC6) into 384-well plates, or loaded as adherent cell layers (TRPC3). True turpentines or resins of *Picea alba* (A, Burgundy resin), *Abies balsamea* (B; Canada balsam), *Larix decidua* (C; larch turpentine), *Pinus spp.* (D, pine resin), propolis (E), *Abies alba* (F; Strassburg turpentine), turpentine resin oil from *Pinus spp.* (G), or a mixture of pine resin and *Larix occidentalis* turpentine (H; Venice turpentine), were serially diluted to the indicated final concentrations, and incubated for 5 min. Fluorescence intensities of fluo-4 were recorded during injection of OAG (50 µM), applying a plate reader device. Relative increases in fluorescence intensities (F/F_0) were obtained, peak intensities after OAG stimulation were determined and normalised to the peak levels that were reached without treatment with turpentines (controls). Shown are means and S.E. of 2-4 independent experiments performed in duplicates, each. Lines represent the result of nonlinear regression analyses, applying a four-parameter Hill equation, or with the sum of two Hill equations (C). Note the larger difference between TRPC6- and TRPC3-blocking properties achieved with the larch turpentine.

Figure 2: Resiniferous compounds that are contained in various conifer turpentines inhibit both TRPC6 and TRPC3.

Experiments were performed essentially as described in Figure 1, but after preincubating cells for 5 min with the indicated non-volatile resin constituents that are generally contained in conifer turpentines, or with the corresponding concentrations of the solvent DMSO. Note the moderate potency and TRPC6 prevalence of inhibition of OAG-induced Ca^{2+} entry.

Molecular Pharmacology Fast Forward. Published on October 23, 2015 as DOI: 10.1124/mol.115.100792
This article has not been copyedited and formatted. The final version may differ from this version.

Figure 3: Isoform-selective inhibition of Ca^{2+} entry through TRPC6 by larixol and larixyl acetate.

The impact of larixol and larixyl acetate on OAG-stimulated Ca^{2+} entry was assessed in fluo-4 loaded $HEK_{hTRPC6\text{-}YFP}$ cells or in $HEK_{hTRPC3\text{-}YFP}$ cells (grey symbols and lines in D and E). Multiwell plates containing fluo-4-loaded $HEK_{hTRPC6\text{-}YFP}$ cells were placed in a fluorescence plate imaging device, and monitored during the sequential application of various concentrations of larixol (A) or larixyl acetate (B), followed by the addition of 50 µM OAG. (C) Representative images of wells, containing fluo-4-loaded HEK_{hTRPC6} cell suspensions imaged before *(1)* and 30 s after *(2)* stimulation with OAG (time points are indicated in panel A and B). The respective concentrations of the modulator or the solvent DMSO in the wells (double determinations) are indicated. (D,E) Concentration response curves were obtained from n = 10-13 independent experiments with $HEK_{hTRPC6\text{-}YFP}$ (black lines) and $HEK_{hTRPC3\text{-}YFP}$ lines (grey lines) and for each modulator, performed as shown in (A-C).

Figure 4: Larixyl acetate does not interfere with the GPCR-induced Ca^{2+} mobilisation and protein kinase C ε (PKCε) translocation.

(A,B) To control for a possible inhibition of the GPCR-induced and phospholipase C-mediated Ca^{2+} mobilisation from $InsP_3$-sensitive stores, parental HEK293 cells were loaded with fluo-4, stimulated with the indicated concentrations of agonists or activators that act on endogenously expressed phospholipase C-activating GPCRs, and Ca^{2+} responses were followed in the presence of 10 µM larixyl acetate (filled symbols) or in solvent controls (open symbols). Shown are means and S.E. of 8 determinations. (C-E) The GPCR-dependent diacylglycerol formation was monitored in living HEK293 cells stably expressing a C-terminally YFP-tagged rat PKCε (PKCε-YFP) as a translocating fluorescent biosensor. (C) Confocal micrographs were taken before (15 s), and during (120 s and 280 s) a combined stimulation with ATP 300 µM, carbachol 1 mM and thrombin 0.5 U/ml. Bars: 20 µm. (D, E) A quantitative analysis of PKCε-YFP translocation was obtained in single cells by determining the percentage of disappearance of fluorescence in regions of interest defined over cytosolic areas. Data represent means and S.E. of 6-8 independent experiments, comprising data of 5-15 cells per imaging experiment.

Molecular Pharmacology Fast Forward. Published on October 23, 2015 as DOI: 10.1124/mol.115.100792
This article has not been copyedited and formatted. The final version may differ from this version.

Figure 5: Isoform-selective block of TRPC, TRPV and TRPM channels by larixol and larixyl acetate.

The impact of larixyl acetate on $[Ca^{2+}]_i$ signals elicited via stimulation of various TRP channel isoforms were assessed in fluo-4 loaded suspensions or adherent cultures of HEK293 cells, stably expressing the following TRP channels: mouse TRPC4β (mTRPC4) or mouse TRPC5 (mTRPC5) stimulated by ATP 300 µM, carbachol 1 mM and thrombin 0.5 U/ml after depleting intracellular Ca^{2+} storage organelles with thapsigargin (2 µM for 5 min), human TRPC7 (hTRPC7) stimulated with 50 µM OAG, rat TRPV1 (rTRPV1) stimulated with 2 µM capasaicin, mouse TRPV4 (mTRPV4) stimulated with 10 nM GSK1016790A, human TRPM2 (hTRPM2) stimulated with 1 mM H_2O_2, mouse TRPM3α_2 (mTRPM3) stimulated with 50 µM pregnenolone sulfate or mouse TRPM8 (mTRPM8) stimulated with 300 µM menthol. Effects of TRPC6 inhibitors were depicted as concentration response curves to inhibit TRPC channels (A). For better comparison, the $HEK_{hTRPC6\text{-}YFP}$ and $HEK_{hTRPC3\text{-}YFP}$ cell data are redrawn. (B) The inhibition of TRPV or TRPM channels by 0.15% DMSO (open bars) or by 15 µM larixyl acetate (filled bars) is depicted as percentage of peak Ca^{2+} responses to the respective activators achieved in a buffer control. With the exception of mTRPM3, none of the differences reached statistical significance. (C) Expression ratios of and FRET efficiencies between TRPC6-YFP and TRPC3-CFP transiently or stably co-expressed in HEK293 cells. (D) Concentration response curve of larixyl acetate effects on OAG (50 µM)-induced $[Ca^{2+}]_i$ signals detected in the stably transfected $HEK_{TRPC6\text{-}YFP:TRPC3\text{-}CFP}$ cell line. Data represent means and S.E. of 2-7 independent experiments, performed in duplicates, each.

Figure 6: Electrophysiological properties of TRPC6 and TRPC3 inhibition by larixyl acetate.

Ionic currents in $HEK_{hTRPC6\text{-}YFP}$ and $HEK_{hTRPC3\text{-}YFP}$ cells were recorded in the whole cell mode by path-clamp analysis. (A) Characteristic TRPC6 currents were elicited by adding 50 µM OAG to the bath solution. Currents were recorded during application of slow voltage ramps from -100 mV to +100 mV (400 mV s^{-1}) as shown in (B). Larixyl acetate was added to the bath solution at the indicated concentrations, and outward (+100 mV; open bars) and inward (-100 mV; black bars) currents through TRPC6 were determined in n = 5-20 cells, and normalized to the cell capacity to obtain current densities (pA pF^{-1}). (B) Examples of leak-corrected I/V ramps in OAG-stimulated $HEK_{hTRPC6\text{-}YFP}$ cells in the absence (black line) and in

Molecular Pharmacology Fast Forward. Published on October 23, 2015 as DOI: 10.1124/mol.115.100792
This article has not been copyedited and formatted. The final version may differ from this version.

the presence of the indicated concentrations of larixyl acetate. (C,D) Statistical analysis of OAG-induced peak outward (open bars) and inward (filled bars) currents measured as shown in (A) in HEK_{hTRPC6} cells (C) or in HEK_{hTRPC3} cells (D; n = 6-16 patched cells). Note the higher test concentrations of larixyl acetate added to $HEK_{hTRPC3\text{-}YFP}$ cells. (E,F) Shown are the corresponding four-parameter Hill equations of current densities of (C,D) with calculated IC_{50} values.

Figure 7: Larixyl acetate acts via an extracellularly accessible binding site in a reversible and repeatable fashion.

(A) $HEK_{hTRPC6\text{-}YFP}$ cells were patched with a pipette solution supplemented with 30 µM AlF_4^- (30 µM $AlCl_3$ and 10 mM NaF) and either no (black line) or 1 µM of larixyl acetate (grey line). Shortly after reaching maximal inward currents (V_{clamp} = -60 mV), 1 µM larixyl acetate was added to the bath solution (outside) as indicated by the bar. Note the maintained response to the extracellularly applied modulator in cells that are intracellularly perfused with larixyl acetate. (B) Statistical analysis of TRPC6 currents measured as shown in (A), or of TRPC6 currents that were elicited by adding 50 µM OAG to the bath solution in cells without intracellular larixyl acetate perfusion (open bars), or in cells that were patched with pipette solutions, containing 1 µM larixyl acetate (grey bars). Filled bars: effect of extracellularly applied larixyl acetate. Means and S.E. of 8-10 experiments are shown. (C) Repeated application and wash-out of 1 µM larixyl acetate to a HEK_{hTRPC6} cell. (D) Magnification of the current decay during acute extracellular addition of 1 µM larixyl acetate and monoexponential fit of the decay kinetic. (E-H) Effects of 1 µM larixyl acetate to OAG-activated TRPC6 currents were tested in excised membrane patches during application to the intracellular surface in inside-out patches (E,F) or to the extracellular surface in outside-out patches (G,H). Shown are representative current traces and open probability (nP_o) analyses, covering consecutive 2-s-bins. Magnified current traces represent time points of basal activity, OAG stimulation and larixyl acetate as indicated by the numbers in the upper left panels. (F,H) Statistical analysis (means and S.E.) of nP_o from 8-10 cells under each condition. Inhibition of OAG-induced increases in nP_o was tested for significance ($p < 0.05$), using Student´s t-test for unpaired data sets.

Molecular Pharmacology Fast Forward. Published on October 23, 2015 as DOI: 10.1124/mol.115.100792
This article has not been copyedited and formatted. The final version may differ from this version.

Figure 8: Effects of larixyl acetate on cell viability, cell proliferation, and maintenance of biological activity after prolonged incubation in full blood

(A-C) HEK293 cells were incubated with the indicated concentrations of larixyl acetate, buffer or solvent controls, and positive test compounds. Membrane integrity (A,B) and cellular metabolic activity (C) were tested by propidium iodide staining and MTT assays, respectively. To induce apoptosis or to directly permeabilize the plasma membrane, 2 µM staurosporine or 50 µM digitonin were applied as controls. Data represent means and S.E. of 3-4 experiments. # significant differences to solvent (DMSO)-treated cells as tested by Student´s t-test for unpaired data. (D) Larixyl acetate was incubated with anticoagulated (11 mM trisodium citrate) human full blood at 37°C for the indicated times. Aliquots were cleared (supernatants of 2,400 g centrifugation), diluted to a final concentration of 10 µM in HBS and added to fluo-4-loaded and thapsigargin-pretreated (2 µM for 5 min) $HEK_{hTRPC6\text{-}YFP}$ cells. A solvent control (0.1% DMSO) was treated and diluted in a similar fashion. TRPC6 activation was induced by adding ATP (300 µM), carbachol (1 mM) and thrombin 0.5 U/ml to stimulate phospholipase C-coupled receptors. Depicted are increases in fluo-4-fluorescence normalised to those observed in the presence of the solvent.

Figure 9: Larixyl acetate blocks OAG-induced increases in $[Ca^{2+}]_i$ but not store depletion-associated Mn^{2+} entry in primary cultures of PASM cells

Primary cultures of rat pulmonary artery smooth muscle (PASM) cells were obtained and maintained without passaging for 5-7 days prior to the experiments. (A) Western blot analysis of TRPC6 and β-actin expression, and immunofluorescence staining of smooth muscle-specific α-actin in cultured PASM cells. Nuclei are counterstained with Hoechst 33342. A micrograph of a representative visual field taken by confocal laser-scanning microscopy is shown. (B) Adherent PASM cells were loaded with fura-2/AM, and subjected to single cell $[Ca^{2+}]_i$ determination, using a digital fluorescence video imaging system. The $[Ca^{2+}]_i$ in PASM cells was recorded during sequential addition of the PKC blocker bisindolylmaleimide-1 (BIM), 100 µM OAG, and 5 µM larixyl acetate (grey line) or no TRPC6 modulator (black line). (C) Experiments as in (B), but with larixyl acetate (1 µM light grey; 5 µM dark grey) or no larixyl acetate (black line) preincubated for 5 min prior to OAG application. Shown are means and S.E. of 7-15 independent experiments. (D) Statistical analysis of basal and the respective OAG-stimulated peak $[Ca^{2+}]_i$ from experiments as shown in (C) #: significant ($p <$

Molecular Pharmacology Fast Forward. Published on October 23, 2015 as DOI: 10.1124/mol.115.100792
This article has not been copyedited and formatted. The final version may differ from this version.

0.05) differences between OAG-stimulated control cells. (E) Manganese quench of fura-2 fluorescence was followed at the isosbestic wavelength of fura-2 (358 nm in our system), after incubating PASM cells with 5 μM larixyl acetate (dark grey), 10 μM lanthanum acetate (La^{3+}, light grey), or the solvent control (0.1% DMSO; black line). Thapsigargin was added to deplete intracellular Ca^{2+} stores and to activate store-operated channels. Note that addition of 300 μM $MnCl_2$ results in a fura-2 quenching, which is inhibited by La^{3+}, but not by larixyl acetate. Data represent means and S.E. of 4 independent determinations, representing 90-160 cells, each. (F) Statistical analysis of 4 independent experiments performed as shown in (E). Depicted are mean fura-2 fluorescence intensities 350 s after the addition of 300 μM $MnCl_2$ to the bath solution. #: statistically significant ($p < 0.05$) differences to thapsigargin-treated control cells in the absence of La^{3+}.

Figure 10: TRPC6-like ionic currents in primary PASM cells are inhibited by larixyl acetate.

Rat PASM cells were obtained as in Fig. 9, but subjected to electrophysiological patch-clamp experiments to measure ionic currents in the whole-cell mode as in Fig. 6. (A,B) Inward and outward currents were measured by repeated application of voltage ramps as depicted in (C,D) during application of 50 μM OAG to the bath solution. Recordings from two representative cells with higher or lower current amplitudes are shown. Time points of voltage ramps shown in (C,D) are indicated in (A,B). (B,D) Larixyl acetate was added to the bath in the continued presence of OAG.

Figure 11: Larixyl acetate blocks the acute hypoxia-induced pulmonary vasoconstriction in mouse lungs.

Mouse lungs were cannulated and perfused with a modified Hanks' balanced salt solution containing no (black line) or 5 μM larixyl acetate (grey line) at a constant flow rate of 50 ml kg^{-1} min^{-1}. (A) The pulmonary artery perfusion pressure (PAP) was measured before (normoxia) and after switching the ventilation from 21% O_2 to a gas mixture containing 1% O_2 (hypoxia). To measure the vascular resistance, the perfusion rate was briefly changed before and after hypoxic ventilation as shown in the lower chart. (B,C) Analysis of perfusion pressure (B) and of vascular resistance (C) during experiments performed as shown in (A). Data represent means and S.E. of 5 independent experiments with and without larixyl

Molecular Pharmacology Fast Forward. Published on October 23, 2015 as DOI: 10.1124/mol.115.100792
This article has not been copyedited and formatted. The final version may differ from this version.

acetate, each. Differences were considered significant ($p < 0.05$) after testing with Mann-Whitney U-test for unpaired (#), and Wilcoxon matched pairs test for paired (*) comparisons.

Molecular Pharmacology Fast Forward. Published on October 23, 2015 as DOI: 10.1124/mol.115.100792
This article has not been copyedited and formatted. The final version may differ from this version.

Tables

Table 1: Half-maximally effective concentrations of various conifer turpentines and their constituents to inhibit TRPC6 or TRPC3.

Half maximally effective concentrations (IC_{50}) of the indicated natural products or compounds were obtained by monitoring OAG (50 μM)-induced increases in Ca^{2+} as shown in Fig. 1-3, and fitting the data to a 4-parameter Hill equation. If half-maximal inhibition was not achieved at the highest test concentration, the IC_{50} was assumed to be higher than the indicated concentration. If responses were augmented, the effect is indicated as positive modulation of Ca^{2+} signals. The ratio of potencies is calculated as IC_{50}(hTRPC3-YFP)/IC_{50}(hTRPC6). Note that high concentrations of essential oils are cytotoxic, and effects may be unrelated to TRPC6 or TRPC3.

Molecular Pharmacology Fast Forward. Published on October 23, 2015 as DOI: 10.1124/mol.115.100792
This article has not been copyedited and formatted. The final version may differ from this version.

		hTRPC6-YFP	*hTRPC3-YFP*	*ratio of potencies*
resins and turpentines	***Burgundy resin***	0.002 g/l	0.007 g/l	3.5-fold
	Canada balsam	0.1 g/l	0.2 g/l	2.0-fold
	larch turpentine	0.013 g/l	0.3 g/l	23.1-fold
	pine resin	0.018 g/l	0.1 g/l	5.6-fold
	propolis	0.014 g/l	0.045 g/l	3.2-fold
	Strassburg turpentine	0.2 g/l	0.68 g/l	3.4-fold
	turpentine resin oil	0.03 g/l	0.11 g/l	3.7-fold
	Venice turpentine	0.14 g/l	0.61 g/l	4.4-fold
essential oils	***Abies alba***	5.9 ml/l	10.7 ml/l	1.8-fold
	Abies sibirica	-	15.8 ml/l	-
	Cedrus atlantica	-	14 ml/l	-
	Cupressus sempervirens	5.0 ml/l	14.2 ml/l	2.8-fold
	Larix decidua	pos. modulator	> 20 ml/l	-
	Pinus cembra	19 ml/l	6.3 ml/l	0.33-fold
	Pinus mugo	pos. modulator	19.2 ml/l	-
	Pinus sylvestris	-	> 20 ml/l	-
resin acids and neutral components	***abietic acid***	21 µM	30 µM	1.4-fold
	neoabietic acid	24 µM	60 µM	2.5-fold
	pimaric acid	25 µM	71 µM	2.8-fold
	isopimaric acid	33 µM	48 µM	1.5-fold
	13-epimanool	10 µM	28.6 µM	2.9-fold
	larixol	2.04 µM	8.32 µM	4.1-fold
	larixyl acetate	0.58 µM	6.83 µM	11.8-fold

Figure 1

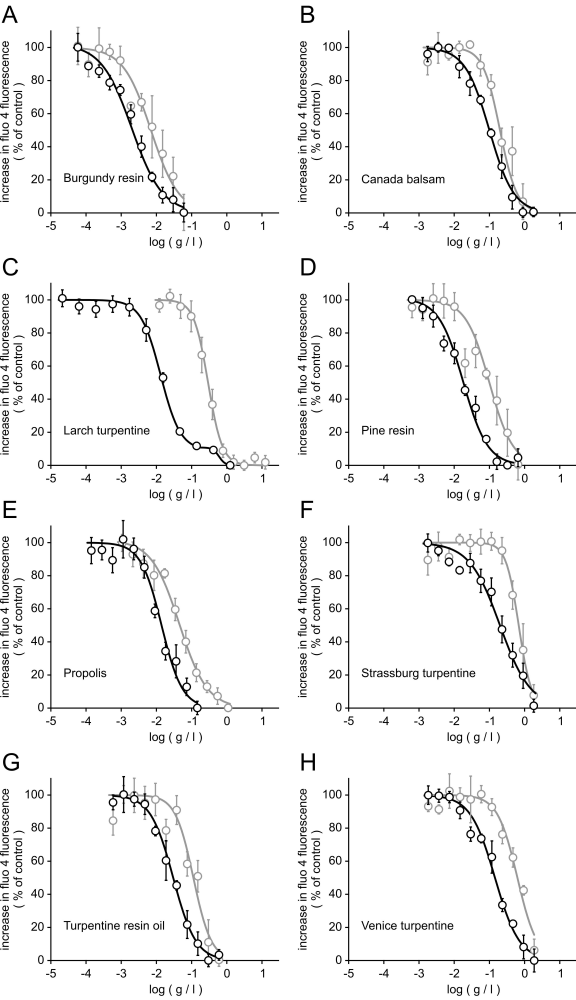
A
B
C
D
E
F
G
H
increase in fluo 4 fluorescence (% of control)
log (g / l)
Burgundy resin
Canada balsam
Larch turpentine
Pine resin
Propolis
Strassburg turpentine
Turpentine resin oil
Venice turpentine

Figure 2

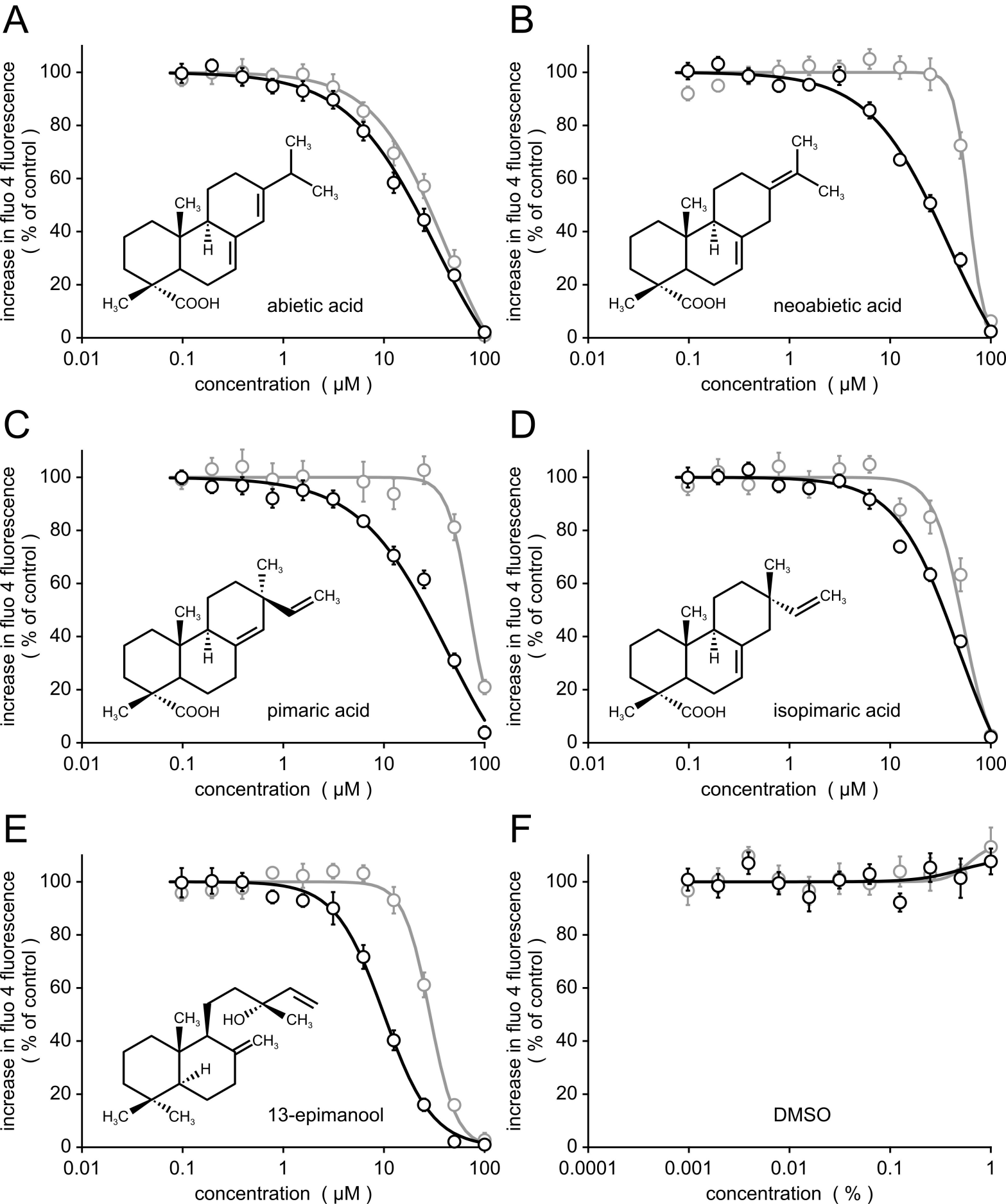
A
B
C
D
E
F
increase in fluo 4 fluorescence (% of control)
concentration (μM)
concentration (%)
abietic acid
neoabietic acid
pimaric acid
isopimaric acid
13-epimanool
DMSO

Figure 3

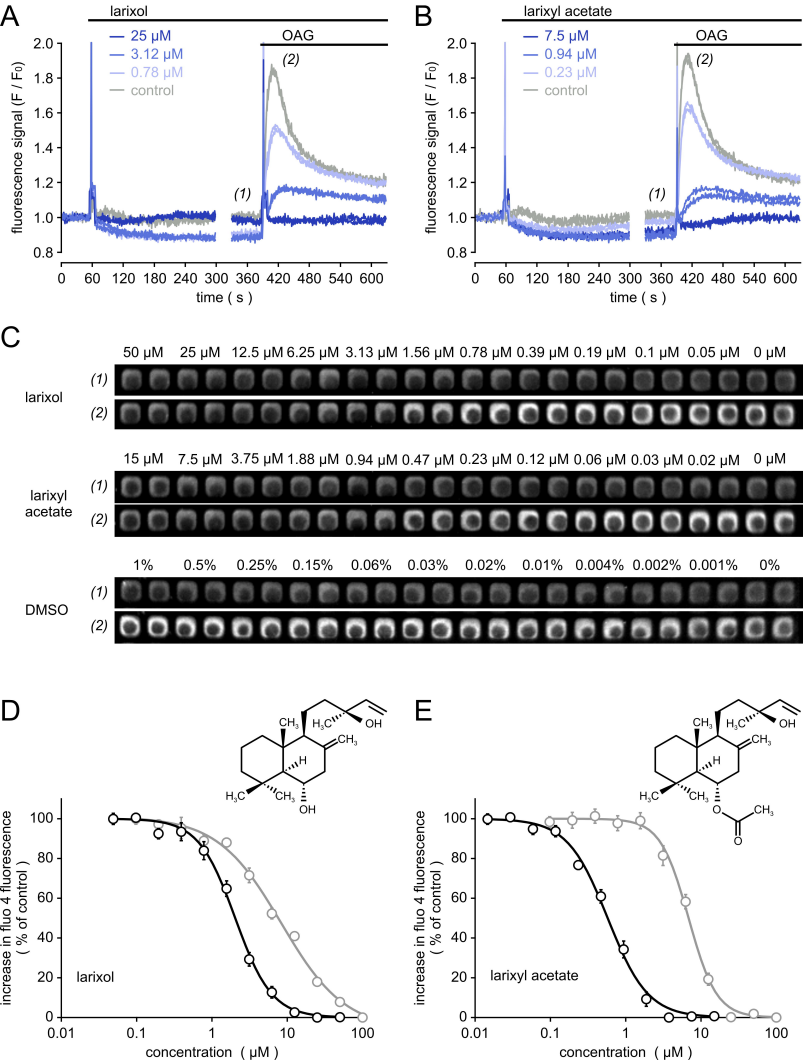
A
larixol
25 μM
3.12 μM
0.78 μM
control
OAG
(1)
(2)
fluorescence signal (F / F0)
time (s)
B
larixyl acetate
7.5 μM
0.94 μM
0.23 μM
control
OAG
(1)
(2)
fluorescence signal (F / F0)
time (s)
C
50 μM 25 μM 12.5 μM 6.25 μM 3.13 μM 1.56 μM 0.78 μM 0.39 μM 0.19 μM 0.1 μM 0.05 μM 0 μM
larixol
(1)
(2)
15 μM 7.5 μM 3.75 μM 1.88 μM 0.94 μM 0.47 μM 0.23 μM 0.12 μM 0.06 μM 0.03 μM 0.02 μM 0 μM
larixyl acetate
(1)
(2)
1% 0.5% 0.25% 0.15% 0.06% 0.03% 0.02% 0.01% 0.004% 0.002% 0.001% 0%
DMSO
(1)
(2)
D
increase in fluo 4 fluorescence (% of control)
larixol
concentration (μM)
E
increase in fluo 4 fluorescence (% of control)
larixyl acetate
concentration (μM)

Figure 4

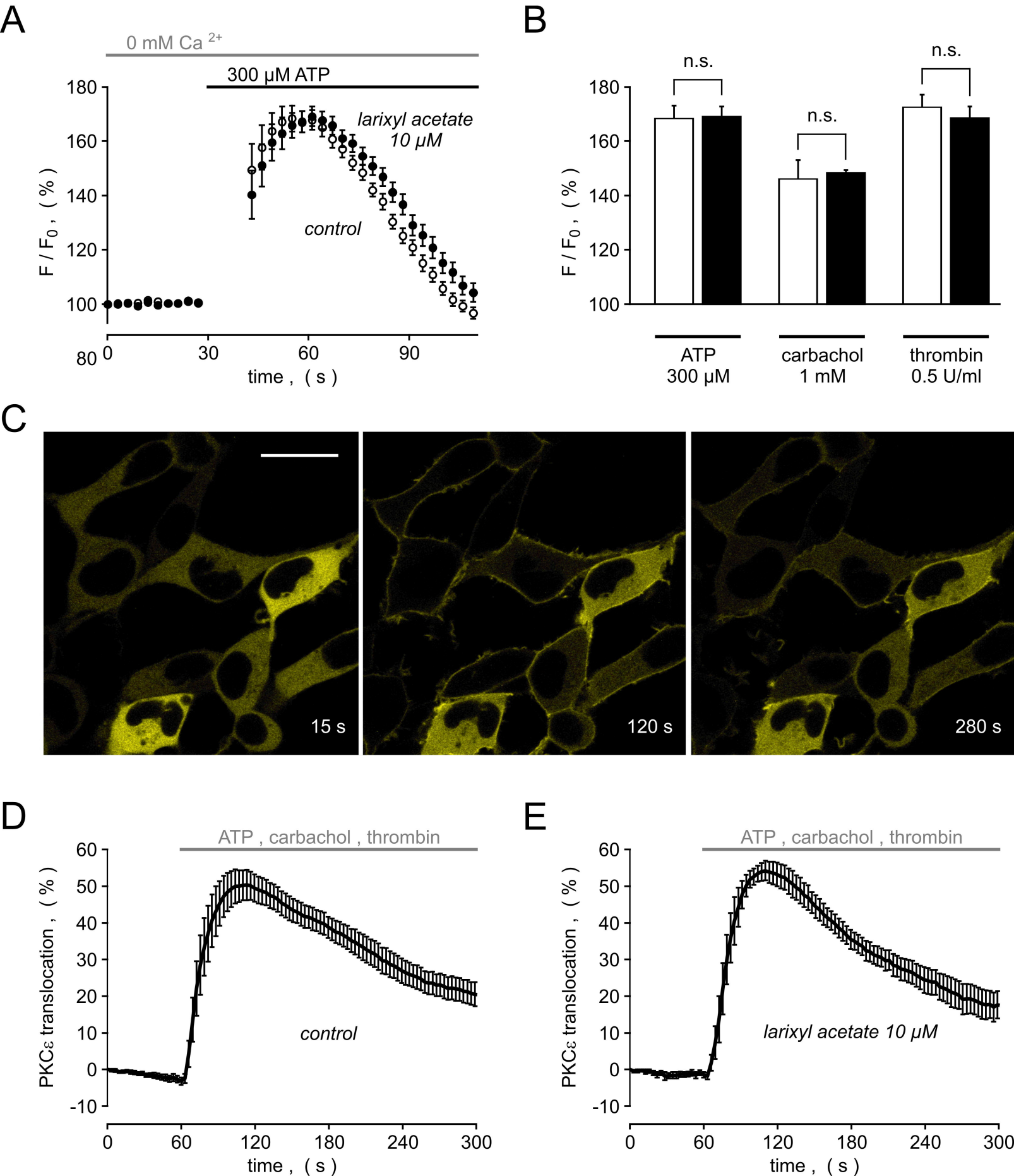
A
0 mM Ca 2+
300 μM ATP
larixyl acetate
10 μM
control
F / F0 , (%)
time , (s)
B
n.s.
n.s.
n.s.
F / F0 , (%)
ATP
300 μM
carbachol
1 mM
thrombin
0.5 U/ml
C
15 s
120 s
280 s
D
ATP , carbachol , thrombin
control
PKCε translocation , (%)
time , (s)
E
ATP , carbachol , thrombin
larixyl acetate 10 μM
PKCε translocation , (%)
time , (s)

Figure 5

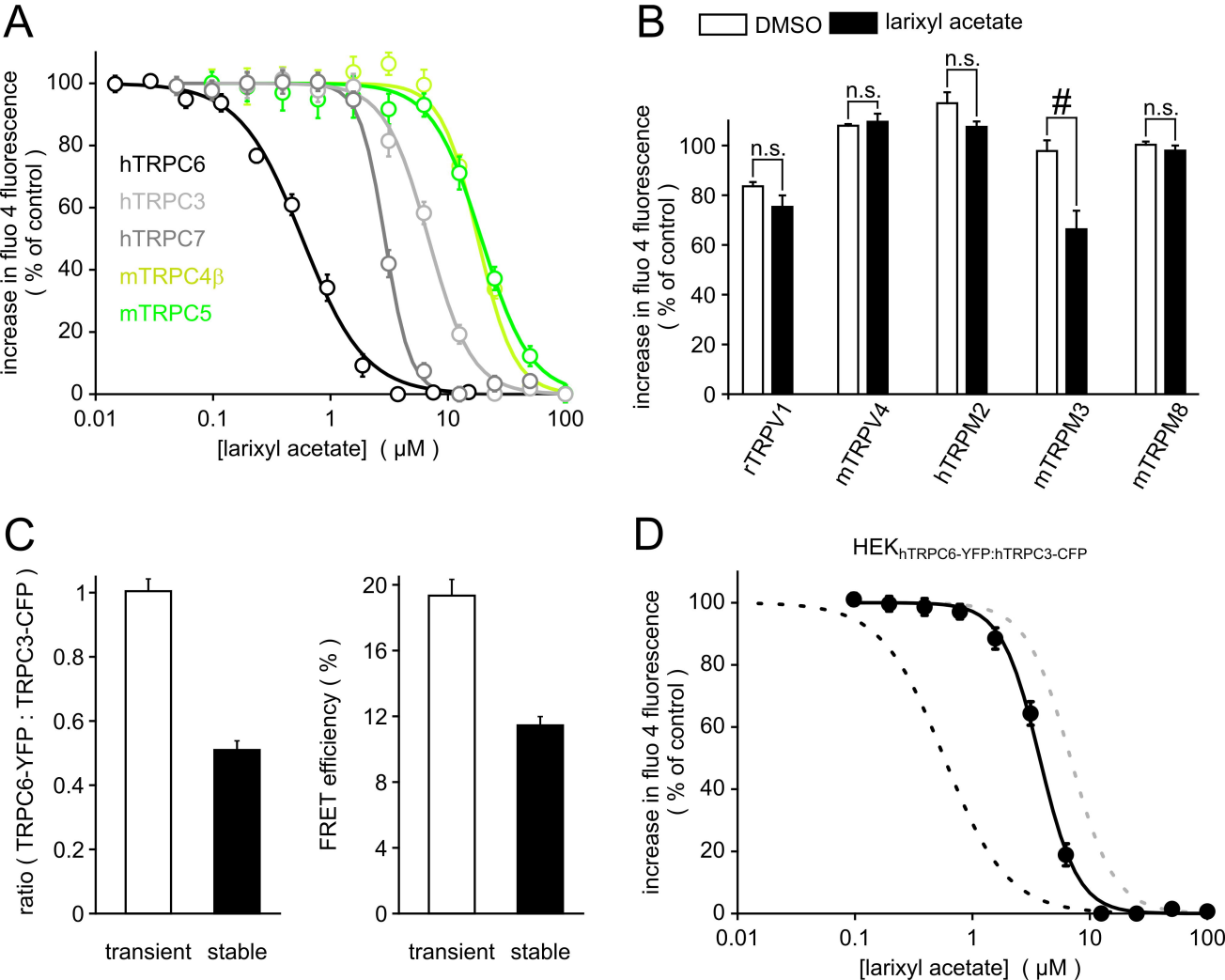
A
increase in fluo 4 fluorescence (% of control)
hTRPC6
hTRPC3
hTRPC7
mTRPC4β
mTRPC5
[larixyl acetate] (μM)
B
DMSO
larixyl acetate
n.s.
#
rTRPV1
mTRPV4
hTRPM2
mTRPM3
mTRPM8
C
ratio (TRPC6-YFP : TRPC3-CFP)
FRET efficiency (%)
transient
stable
D
HEK hTRPC6-YFP:hTRPC3-CFP

Figure 6

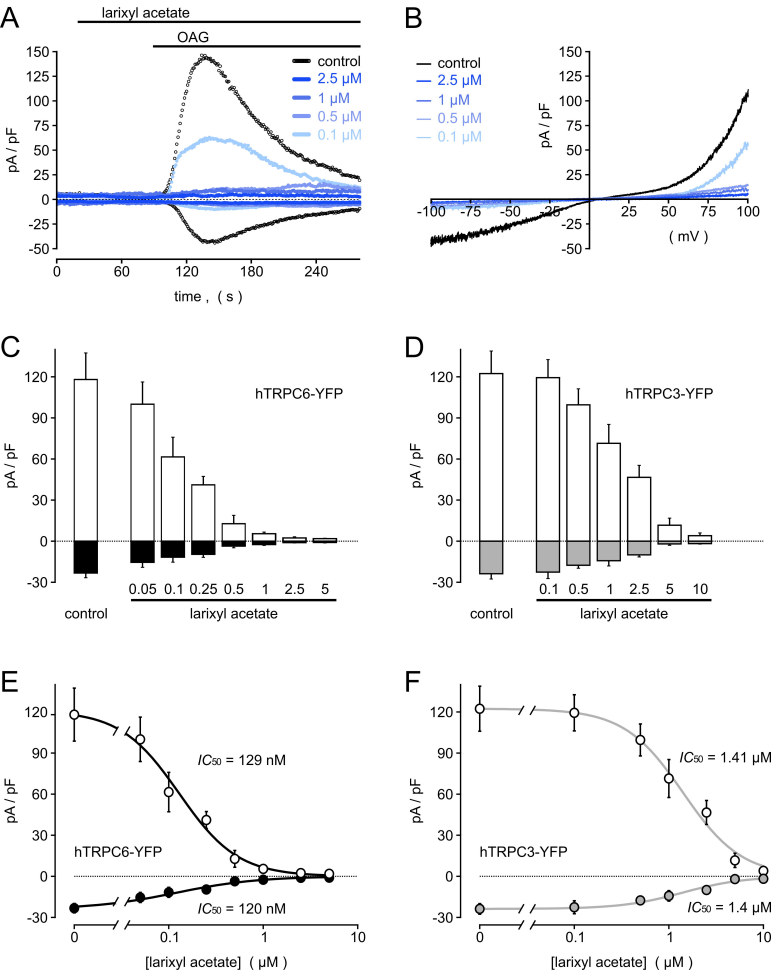
A
larixyl acetate
OAG
control
2.5 μM
1 μM
0.5 μM
0.1 μM
pA / pF
time , (s)
B
control
2.5 μM
1 μM
0.5 μM
0.1 μM
pA / pF
(mV)
C
hTRPC6-YFP
pA / pF
0.05 0.1 0.25 0.5 1 2.5 5
control
larixyl acetate
D
hTRPC3-YFP
pA / pF
0.1 0.5 1 2.5 5 10
control
larixyl acetate
E
IC50 = 129 nM
hTRPC6-YFP
IC50 = 120 nM
pA / pF
[larixyl acetate] (μM)
F
IC50 = 1.41 μM
hTRPC3-YFP
IC50 = 1.4 μM
pA / pF
[larixyl acetate] (μM)

Figure 7

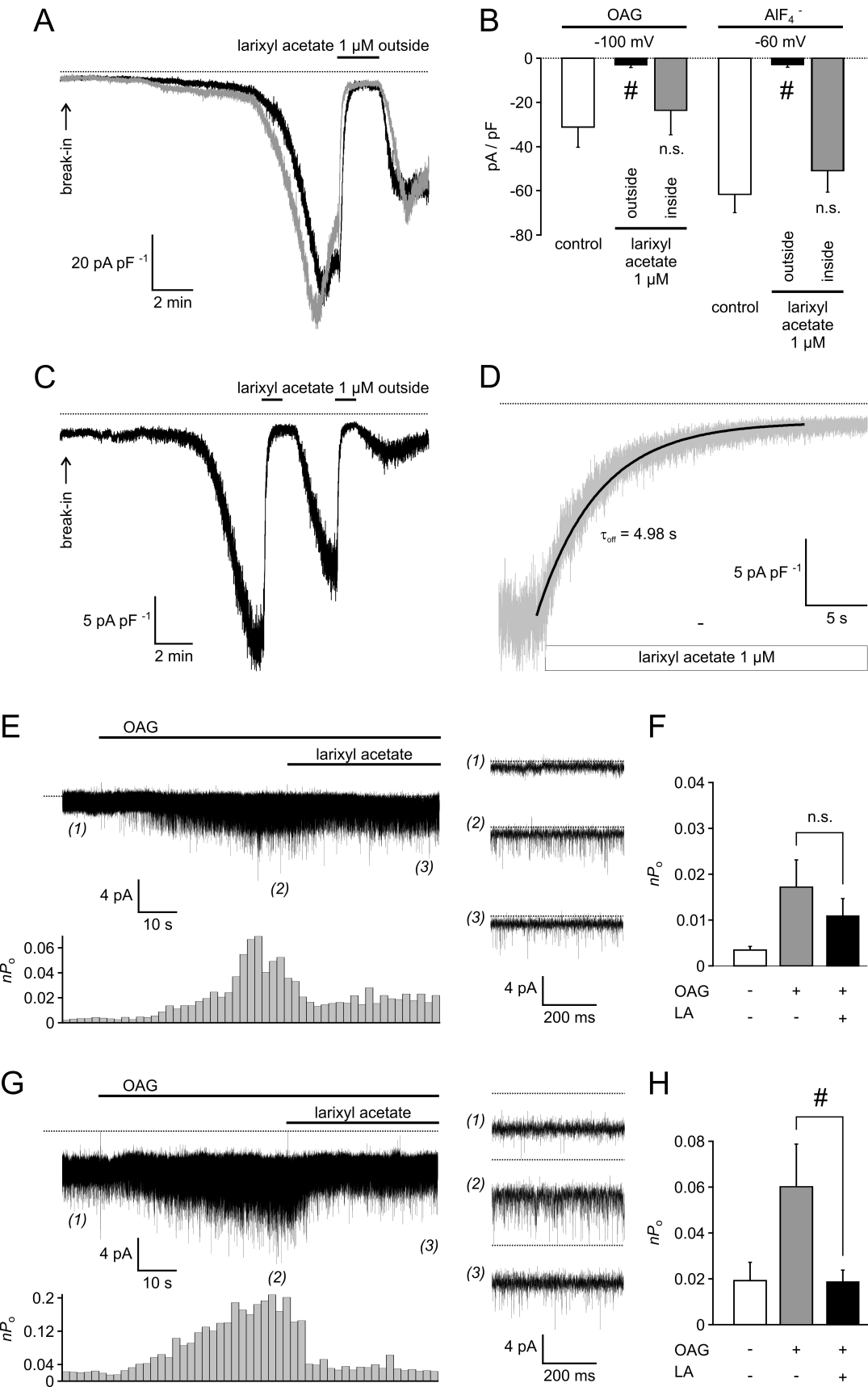
A
larixyl acetate 1 µM outside
break-in
20 pA pF -1
2 min
B
OAG
-100 mV
AlF4 -
-60 mV
pA / pF
0
-20
-40
-60
-80
#
n.s.
outside
inside
control
larixyl acetate 1 µM
C
larixyl acetate 1 µM outside
break-in
5 pA pF -1
2 min
D
τoff = 4.98 s
5 pA pF -1
5 s
larixyl acetate 1 µM
E
OAG
larixyl acetate
(1)
(2)
(3)
4 pA
10 s
nPo
0.06
0.04
0.02
0
4 pA
200 ms
F
0.04
0.03
0.02
0.01
0
n.s.
nPo
OAG - + +
LA - - +
G
OAG
larixyl acetate
(1)
(2)
(3)
4 pA
10 s
nPo
0.2
0.12
0.04
0
4 pA
200 ms
H
#
0.08
0.06
0.04
0.02
0
nPo
OAG - + +
LA - - +

Figure 8

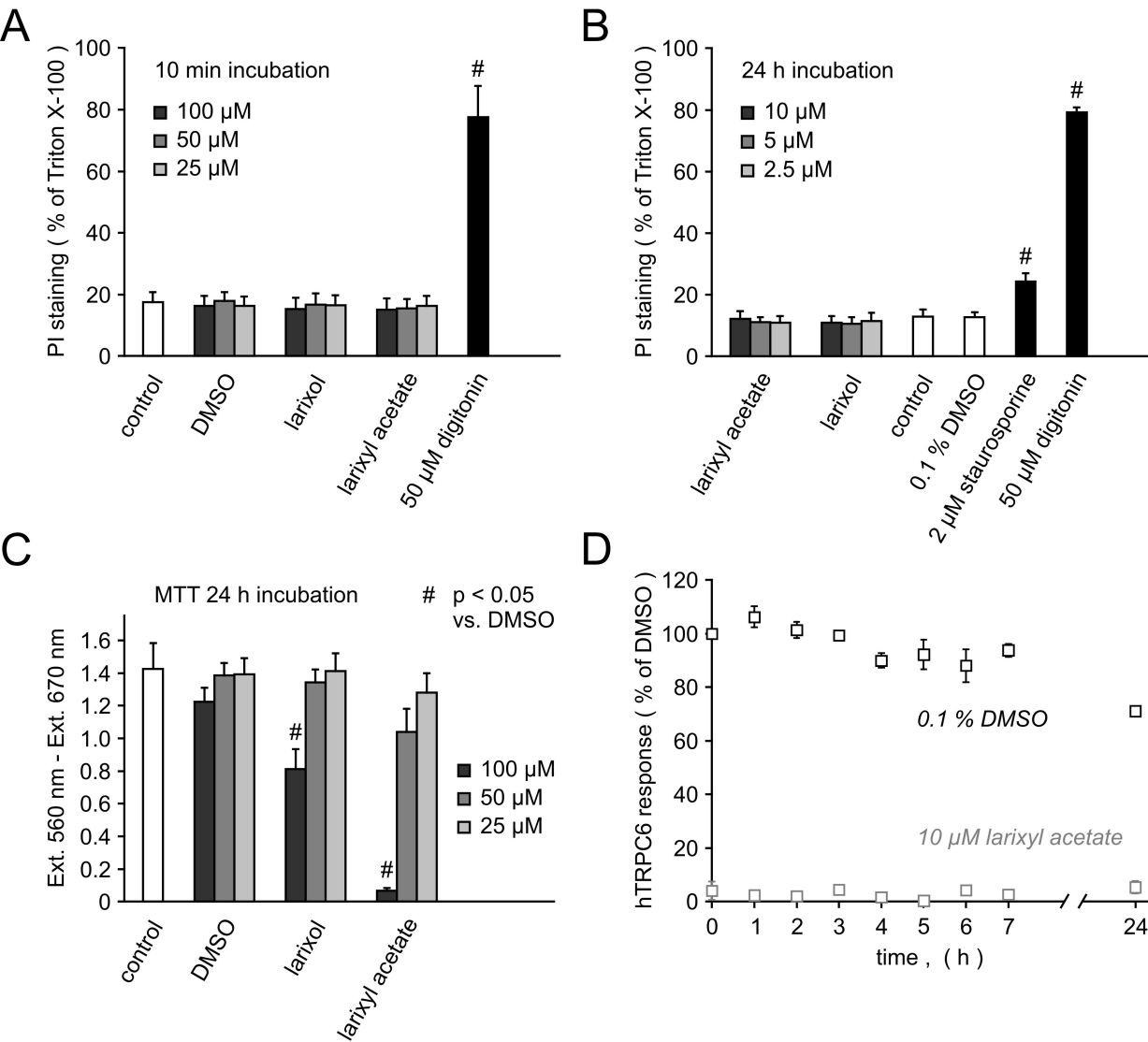
A
10 min incubation
100 µM
50 µM
25 µM
PI staining (% of Triton X-100)
control
DMSO
larixol
larixyl acetate
50 µM digitonin
B
24 h incubation
10 µM
5 µM
2.5 µM
PI staining (% of Triton X-100)
larixyl acetate
larixol
control
0.1 % DMSO
2 µM staurosporine
50 µM digitonin
C
MTT 24 h incubation
# p < 0.05
vs. DMSO
Ext. 560 nm - Ext. 670 nm
100 µM
50 µM
25 µM
control
DMSO
larixol
larixyl acetate
D
hTRPC6 response (% of DMSO)
0.1 % DMSO
10 µM larixyl acetate
time , (h)

Figure 9

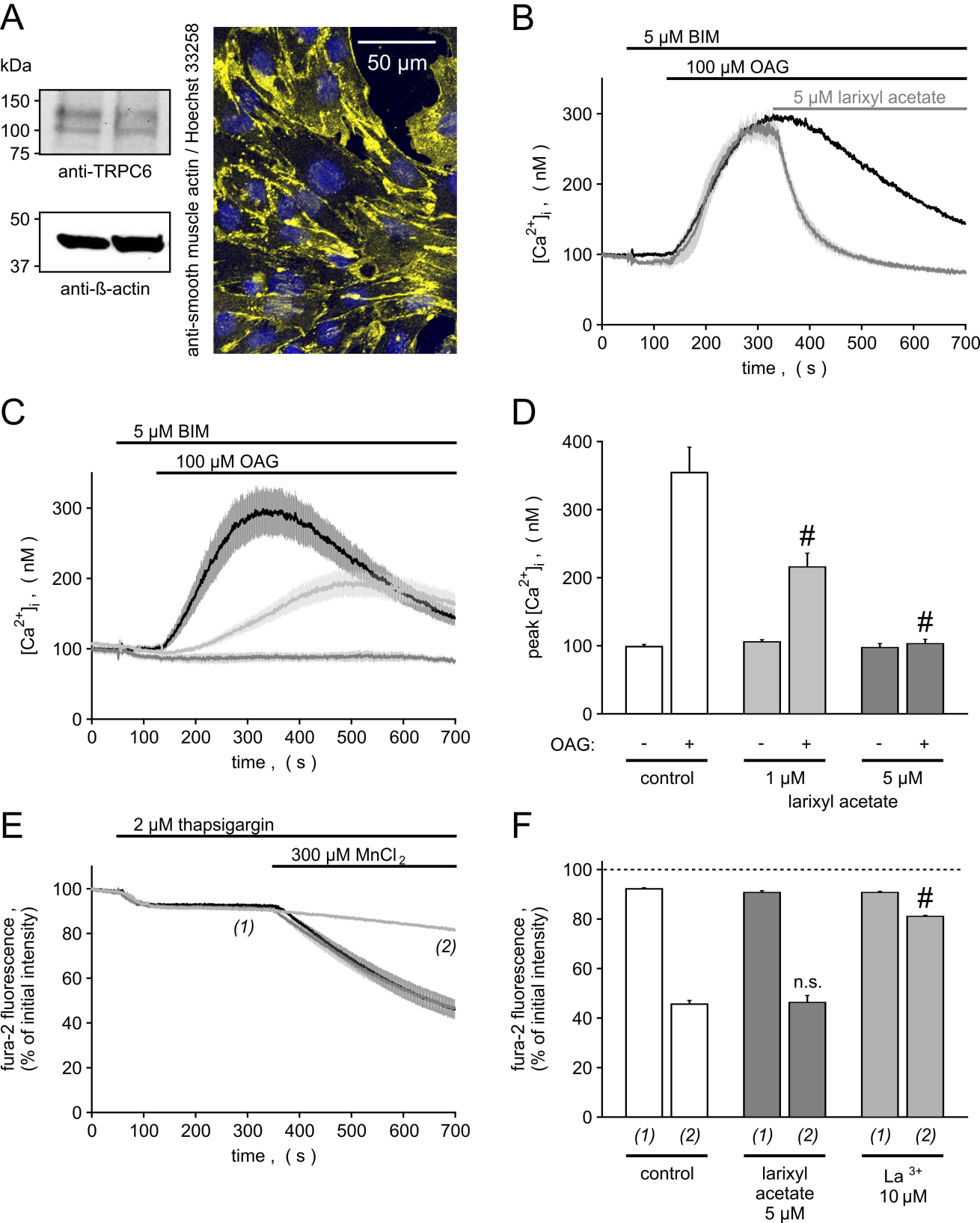
A
kDa
150
100
75
anti-TRPC6
50
37
anti-ß-actin
anti-smooth muscle actin / Hoechst 33258
50 µm
B
5 µM BIM
100 µM OAG
5 µM larixyl acetate
[Ca2+]i , (nM)
time , (s)
C
5 µM BIM
100 µM OAG
[Ca2+]i , (nM)
time , (s)
D
peak [Ca2+]i , (nM)
#
#
OAG:
control
1 µM
larixyl acetate
5 µM
E
2 µM thapsigargin
300 µM MnCl2
(1)
(2)
fura-2 fluorescence ,
(% of initial intensity)
time , (s)
F
fura-2 fluorescence ,
(% of initial intensity)
#
n.s.
(1)
(2)
control
larixyl
acetate
5 µM
La 3+
10 µM

Figure 10

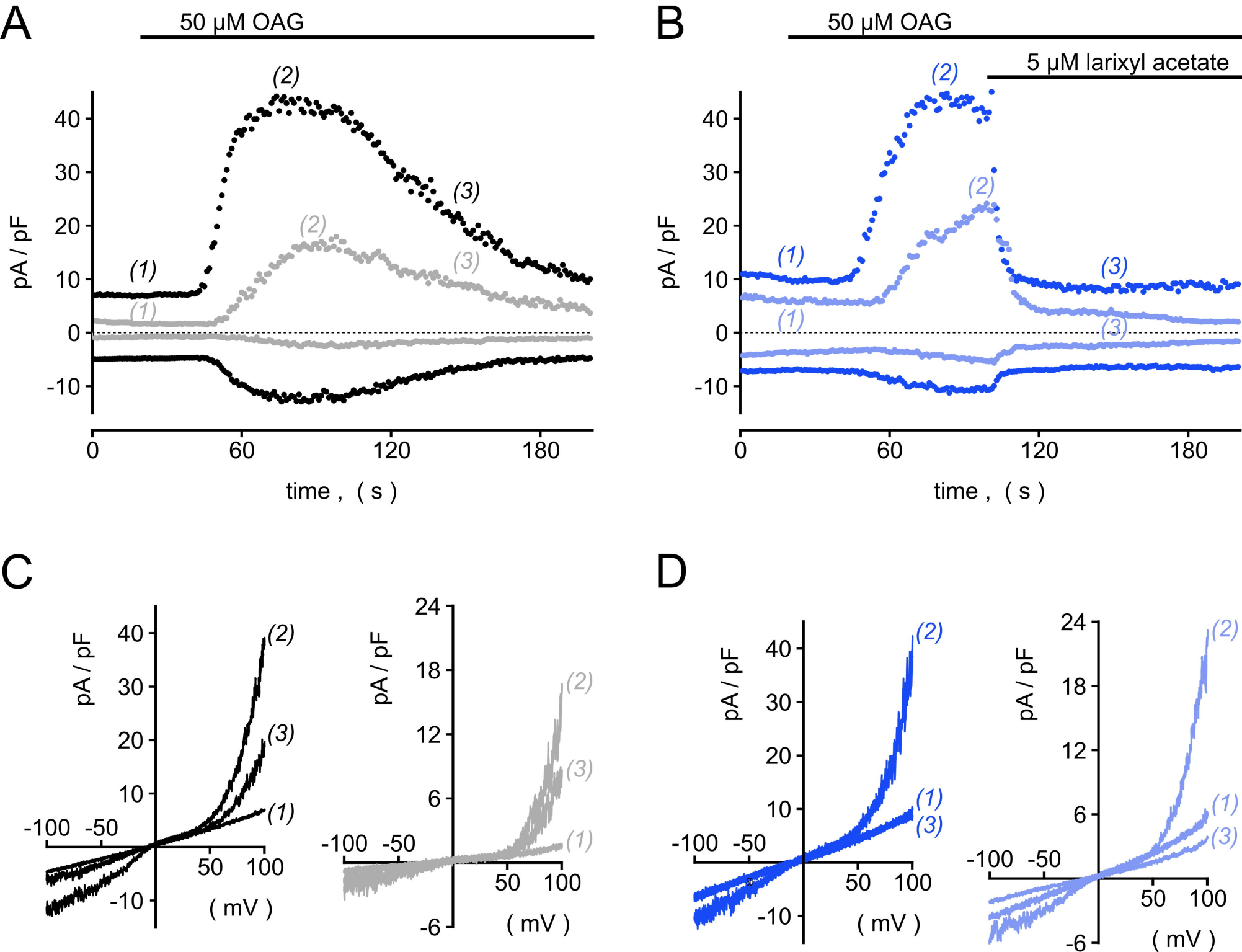
A
50 μM OAG
(2)
(3)
(1)
(2)
(3)
(1)
40
30
20
10
0
-10
pA / pF
0
60
120
180
time , (s)
B
50 μM OAG
5 μM larixyl acetate
(2)
(2)
(1)
(3)
(1)
(3)
40
30
20
10
0
-10
pA / pF
0
60
120
180
time , (s)
C
pA / pF
40
30
20
10
-10
(2)
(3)
(1)
-100
-50
50
100
(mV)
pA / pF
24
18
12
6
-6
(2)
(3)
(1)
-100
-50
50
100
(mV)
D
pA / pF
40
30
20
10
-10
(2)
(1)
(3)
-100
-50
50
100
(mV)
pA / pF
24
18
12
6
-6
(2)
(1)
(3)
-100
-50
50
100
(mV)

Figure 11

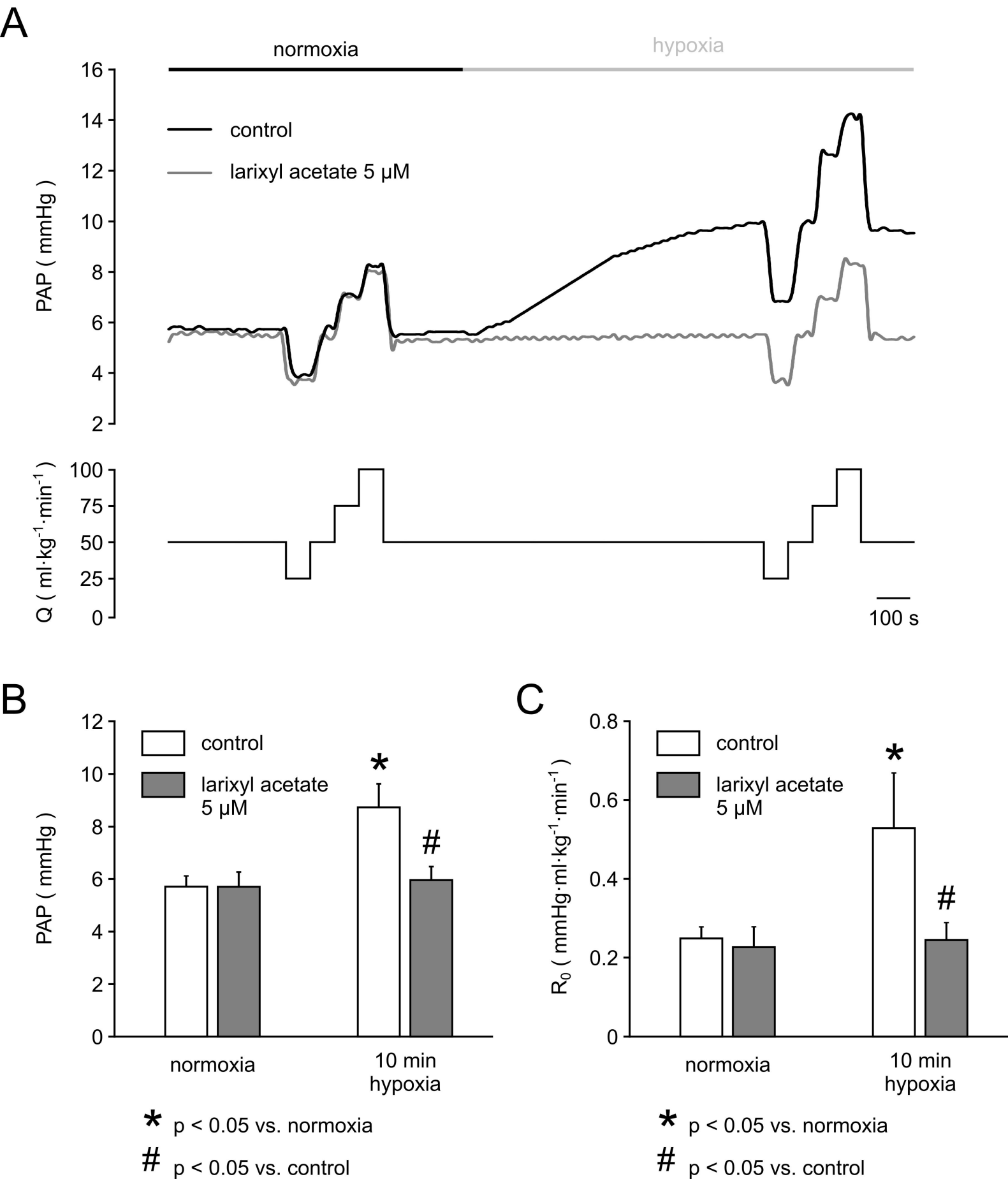
A
normoxia
hypoxia
control
larixyl acetate 5 µM
PAP (mmHg)
16
14
12
10
8
6
4
2
Q (ml·kg-1·min-1)
100
75
50
25
0
100 s
B
control
larixyl acetate 5 µM
PAP (mmHg)
12
10
8
6
4
2
0
*
#
normoxia
10 min hypoxia
* p < 0.05 vs. normoxia
# p < 0.05 vs. control
C
control
larixyl acetate 5 µM
R0 (mmHg·ml·kg-1·min-1)
0.8
0.6
0.4
0.2
0
*
#
normoxia
10 min hypoxia
* p < 0.05 vs. normoxia
# p < 0.05 vs. control

Supplemental Figures to:

Identification and validation of larixyl acetate as a potent TRPC6 inhibitor

Nicole Urban, Liming Wang, Sandra Kwiek, Jörg Rademann,
Wolfgang M. Kuebler, and Michael Schaefer

Molecular Pharmacology

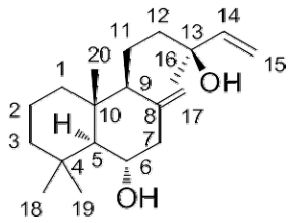

Supplemental Figure 1: Structure and chemical characterisation of Larixol

R_f = 0.02 (Hexan: EE 9:1 (v:v)

T_m = 100°C

^{1}H-NMR (300 MHz, $CDCl_3$) δ [ppm] = 0.68 (s, 3H, 20- C**H_3**), 0.99 (s, 3H, 18/19-C**H_3**), 1.01-1.60 (m, 12H), 1.16 (s, 3H, 18/19-C**H_3**), 1.13 (d, 1H, 5-C**H**), 1.26 (s, 3H, 16-C**H_3**), 2.04 (t, 1H, 7-C**H**), 2.66 (dd, 1H, 7-C**H**), 3.82 (dt, 1H, 6-C**H**), 4.65 (dd, 2H, 17- C**H_2**), 5.04 (dd, 1H, 15-C**H**, J_{cis} = 10.37 Hz, $J_{geminal}$ = 1.26 Hz), 5.18 (dd,1H, 15-C**H**, J_{trans} = 17.37 Hz, $J_{geminal}$ = 1.26 Hz), 5.89 (dd, 1H, 14-C**H,** J_{trans} = 17.37 Hz, J_{cis} = 10.37 Hz)

^{13}C-NMR (75 MHz, $CDCl_3$) δ [ppm] = 16.3 (20-**C**H_3), 18.3 (11-**C**H_2), 19.4 (2-**C**H_2), 22.6 (18/19-**C**H_3), 28.0 (16-**C**H_3), 34.1 (4-**C**), 36.9 (18/19-**C**H_3), 39.6 (1-**C**H_2), 39.8 (10-**C**H_2), 41.6 (12-**C**H_2), 44.0 (3-**C**H_2), 49.4 (7-**C**H_2), 56.7 (9-**C**H), 60.8 (5-**C**H), 71.9 (6-**C**H), 73.8 (13-**C**), 108.6 (17-**C**H_2), 111.9 (15-**C**H_2), 145.4 (14-**C**H), 145.8 (8-**C**)

HRMS [M+Na^+] calculated 329.24565 Da, found 329.24510 m/z.

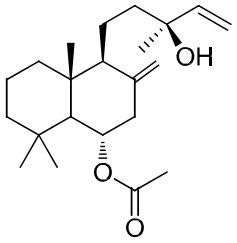

Supplemental Figure 2: Structure and chemical characterisation of larix-6-yl monoacetate

R_f = 0.30 (Hexan: EE 4:1(v:v))

^{1}H-NMR (300 MHz, $CDCl_3$) δ [ppm] = 0.73 (s, 3H, 20- C**H_3**), 0.83 (s, 3H, 18/19-C**H_3**), 1.00 (s, 3H, 18/19-C**H_3**), 1.03-1.80 (m, 12H), 1.26 (s, 3H, 16-C**H_3**), 1.40 (d, 1H, 5-C**H**), 2.02 (s, 3H, Ac-C**H_3**), 2.66 (dd, 1H, 7-C**H**), 4.63 (m, 1H, 17-C**H_2**),), 4.91 (m, 1H,17-C**H_2**), 4.97-5.06 (m, 2H,), 5.19 (dd,1H, 15-C**H**), 5.89 (dd, 1H, 14-C**H**)

^{13}C-NMR (75 MHz, $CDCl_3$) δ [ppm] = 16.2 (20-**C**H_3), 18.2 (11-**C**H_2), 19.2 (2-**C**H_2), 22.2 (Ac-**C**H_3), 22.7 (18/19-**C**H_3), 28.0 (16-**C**H_3), 33.7 (4-**C**), 36.4 (18/19-**C**H_3), 39.3 (1-**C**H_2), 40.1 (10-**C**H_2), 41.5 (12-**C**H_2), 43.7 (3-**C**H_2), 44.4 (7-**C**H_2), 56.6 (9-**C**H), 57.8 (5-**C**H), 73.5 (6-**C**H), 73.7 (13-**C**), 109.7 (17-**C**H_2), 111.9 (15-**C**H_2), 144.5 (14-**C**H), 145.4 (8-**C**), 170.3 (Ac-**C**O)

HRMS [M+Na^+] calculated 371.25621 Da, found 371.25567 m/z

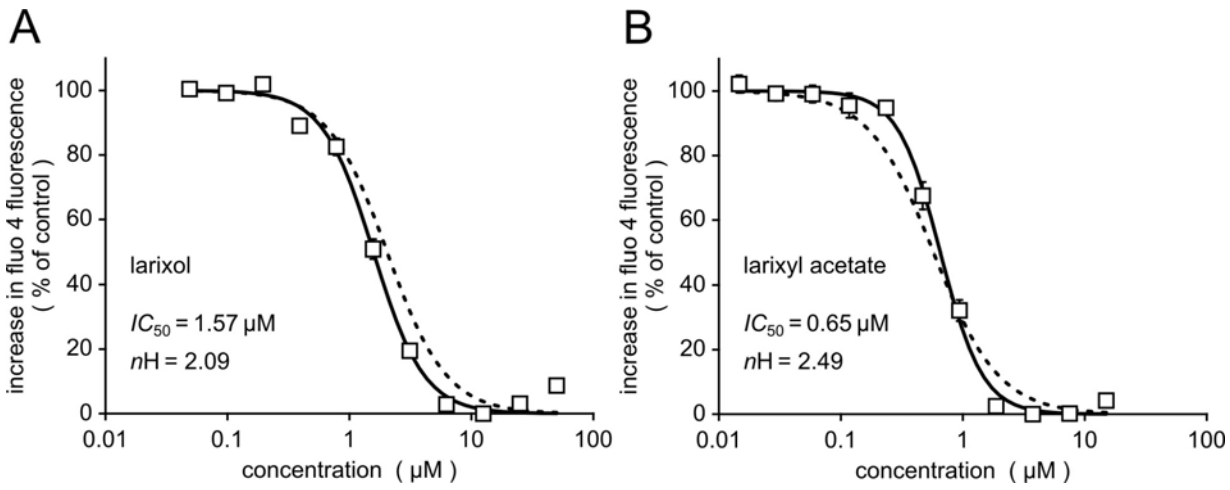

Supplemental Figure 3: Potency of larixol and larixyl acetate to inhibit Ca^{2+} entry through TRPC6 in the receptor-induced mode of activation.

To assess whether the TRPC6 inhibitors are effective when TRPC6 is activated in a receptor-mediated fashion, fluo-4-loaded HEK_{hTRPC6} cells were preincubated for 5 min with 2 µM thapsigargin in the presence of various concentrations of larixol (A) or larixyl acetate (B), and then stimulated with ATP (300 µM), carbachol (1 mM), and thrombin (0.5 U/ml) to induce activation of endogenous phospholipase C. Concentration-response curves were fitted to a four parameter Hill equation, and resulting IC_{50} and Hill coefficients are indicated. For comparison, the concentration response curve of TRPC6 inhibition in the OAG-activated mode (Fig. 3D,E of the main manuscript) is superimposed as dashed lines.

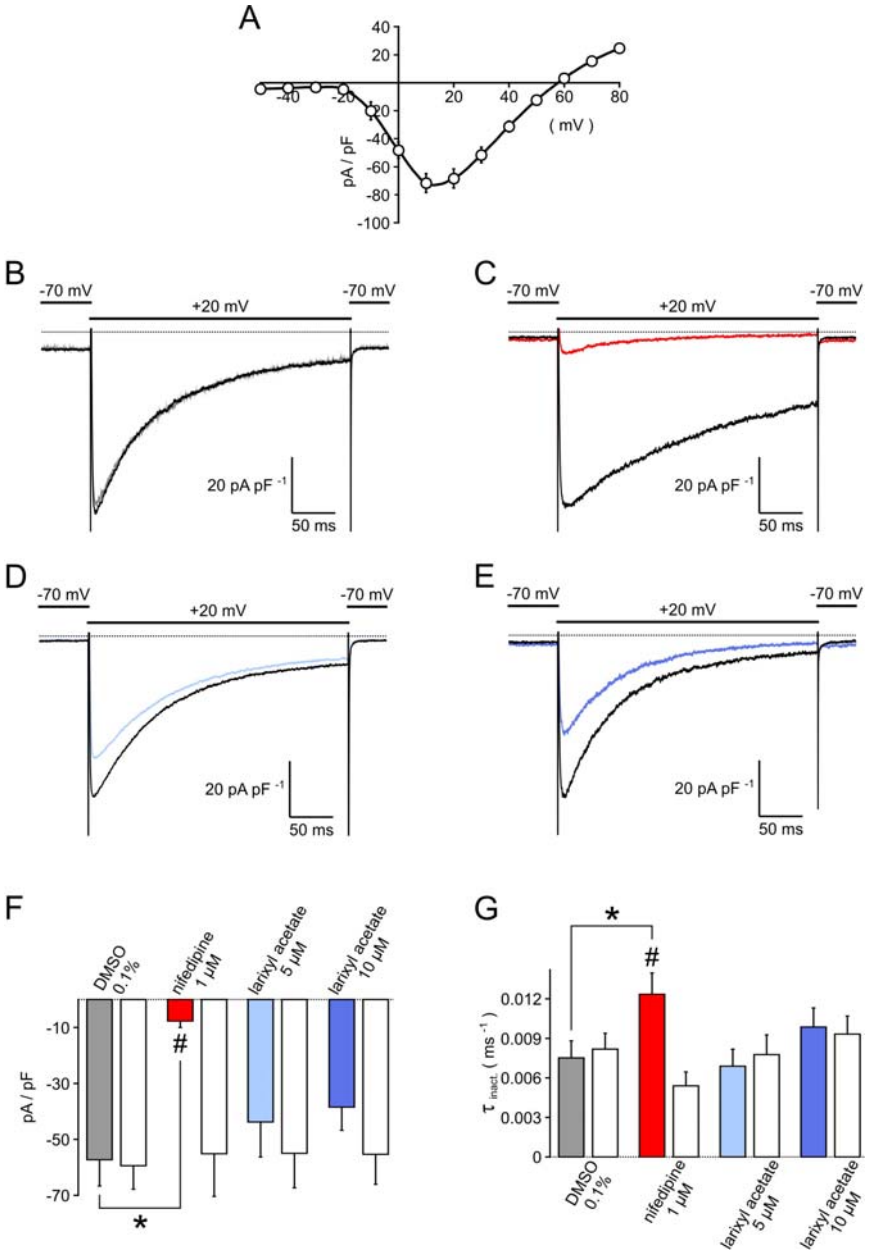

Supplemental Figure 4: Effect of larixyl acetate on voltage-gated Ca^{2+} channels ($Ca_V1.2$).

HEK293 cells were transiently transfected with expression plasmids encoding the $\alpha 1_{c77}$, the β_{2a}, and the $\alpha_{2\delta}$ subunits of $Ca_V1.2$ along with a yellow fluorescent protein as transfection marker. (A) Ba^{2+} currents through recombinant $Ca_V1.2$ channels were measured in voltage step protocols, after stepping from a holding potential of -70 mV to the indicated voltages. Shown are means and S.E. of peak current amplitudes determined in 20 patched cells. (B-E) Superposition of depolarisation-induced Ba^{2+} currents in the presence of the indicated modulators, and 160 s after their wash-out (black lines). (F,G) Statistical analysis of modulator effects on peak current densities (F) and on inactivation time constants $\tau_{inact.}$ (monoexponential fits; G) calculated from 6-9 experiments performed as shown in (B-E). Filled bars: values in the presence of the indicated modulators; open bars: values after wash-out of the respective modulator.